

1 **High throughput genotyping of structural variations in a**
2 **complex plant genome using an original Affymetrix®**
3 **Axiom® array**
4

5 Clément Mabire^{2*}, Jorge Duarte^{1*}, Aude Darracq², Ali Pirani³, Hélène Rimbert^{1,4}, Delphine Madur²,
6 Valérie Combes², Clémentine Vitte², Sébastien Praud¹, Nathalie Rivière¹, Johann Joets², Jean-Philippe
7 Pichon¹, Stéphane D. Nicolas²

8 *Two authors contributed equally to work

9 Authors Affiliation:

10 1 Biogemma - Centre de Recherche de Chappes, CS 90126, Chappes 63720, France

11 2 GQE – Le Moulon, INRA, Univ. Paris-Sud, CNRS, AgroParisTech, Université Paris-Saclay, 91190 Gif-sur-
12 Yvette, France

13 3 Thermo Fisher Scientific, 3450 Central Expressway, Santa Clara, CA, 95051, USA

14 4 Present address: GDEC, INRA, Université Clermont Auvergne, 63000 Clermont-Ferrand, France

15 Corresponding authors: stephane.nicolas@inra.fr

16

17

18

19 Abstract

20 **Background**

21 Insertions/deletions (InDels) and more specifically presence/absence variations (PAVs) are pervasive in
22 several species and have strong functional and phenotypic effect by removing or drastically modifying
23 genes. Genotyping of such variants on large panels remains poorly addressed, while necessary for
24 approaches such as association mapping or genomic selection.

25 **Results**

26 We have developed, as a proof of concept, a new high-throughput and affordable approach to genotype
27 InDels. We first identified 141,000 InDels by aligning reads from the B73 line against the genome of three
28 temperate maize inbred lines (F2, PH207, and C103) and reciprocally. Next, we designed an Affymetrix®
29 Axiom® array to target these InDels, with a combination of probes selected at breakpoint sites (13%) or
30 within the InDel sequence, either at polymorphic (25%) or non-polymorphic sites (63%) sites. The final
31 array design is composed of 662,772 probes and targets 105,927 InDels, including PAVs ranging from 35bp
32 to 129kbp. After Affymetrix® quality control, we successfully genotyped 86,648 polymorphic InDels (82%
33 of all InDels interrogated by the array) on 445 maize DNA samples with 422,369 probes. Genotyping InDels
34 using this approach produced a highly reliable dataset, with low genotyping error (~3%), high call rate
35 (~98%), and high reproducibility (>95%). This reliability can be further increased by combining genotyping
36 of several probes calling the same InDels (<0.1% error rate and >99.9% of call rate for 5 probes). This
37 “proof of concept” tool was used to estimate the kinship matrix between 362 maize lines with 57,824
38 polymorphic InDels. This InDels kinship matrix was highly correlated with kinship estimated using SNPs
39 from Illumina 50K SNP arrays.

40 **Conclusions**

41 We efficiently genotyped thousands of small to large InDels on a sizeable number of individuals using a
42 new Affymetrix® Axiom® array. This powerful approach opens the way to studying the contribution of
43 InDels to trait variation and heterosis in maize. The approach is easily extendable to other species and
44 should contribute to decipher the biological impact of InDels at a larger scale.

45

46 **Keywords**

47 Present Absent Variation, Copy Number Variation, Structural Variation, genotyping, array, Zea mays,
48 Genome assembly, Breakpoint, Chromosomal rearrangements

49

50 **Background**

51 In the past decade, there has been growing evidence that structural variations (SVs) are pervasive
52 within plant genomes [1–9]. Insertion/deletions (InDels) are one class of SVs of particular interest, since
53 they lead to the presence or absence of, sometimes large, genomic regions at a given locus, among
54 individuals from the same species. The content of these InDels can be present elsewhere in the genome,
55 but they can also be completely absent from the genome, in which case they are referred to as
56 presence/absence variants (PAVs). Some InDels carry entire genes or affect gene regulatory elements and
57 are thus likely to have a functional and phenotypic impact [10–12, 7, 13]. Hundreds to thousands of SVs,
58 including PAVs and copy number variations (CNVs), have been discovered in several plant species,
59 including wheat [14], rice [15], *Arabidopsis thaliana* [13], potato [16], pigeon peas [17], and sorghum [18].
60 These results support the idea that one single reference genome cannot properly represent the complete
61 gene set of a given species. There has been an increasing interest for building new individual genomes in
62 complement to the reference genome, in order to better describe the genetic diversity within a plant
63 species [3, 19–25].

64 In maize, BAC sequence comparison first revealed that gene and transposable element content
65 greatly vary between inbred lines [26, 27]. Whole genome sequencing of the B73 inbred line then provided
66 the opportunity to explore the extent of SVs across the entire maize genome [28] by designing
67 Comparative Genomic Hybridization (CGH) technology [29]. Several CGH studies found multiple CNVs
68 between the B73 reference genome and other maize inbred lines or teosintes [2, 8, 9]. These studies
69 demonstrated the large extent of SVs among maize inbred lines, including presence/absence variations of
70 low copy sequences, such as genes. This was well illustrated by the discovery of a large 2 Mbp
71 presence/absence region between Mo17 and B73 carrying several genes [2, 9, 20, 21]. However, CGH
72 array technology shows several major drawbacks since (i) it does not allow the discovery of sequences
73 that are not present in the reference genome used for designing probes of the arrays, (ii) it has a limited
74 resolution which does not allow detection of InDels smaller than 1kb, and (iii) it is costly and labor-
75 intensive, and therefore not adapted for genotyping several hundreds of individuals.

76 Methods based on SNP array experiments have been developed to detect CNVs and were shown
77 to be more affordable and with higher throughput than CGH arrays [32–35]. Didion et al. (2012) identified
78 atypical patterns of reduced hybridization intensities that were highly reproducible, so called “off-target
79 variants” (OTVs) [36]. OTV patterns could originate either from the absence of the sequence due to a PAV
80 polymorphism, or to a single nucleotide polymorphism within the probe sequence, thus preventing the
81 correct hybridization of the DNA sample. For instance, 45,974 OTVs were discovered in a maize population
82 using the 600K Affymetrix® Axiom® SNP array [37]. While these approaches proved to be useful, there is
83 a strong risk of false positive detection of PAVs using OTV patterns, mainly because these arrays were not
84 designed to target PAVs. In order to reduce this risk of false positive detection of PAVs and more largely
85 CNVs, several methods based either on segmentation or Hidden Markov Chain have been developed to
86 use variation of fluorescent intensity signal of contiguous probes along the genome [38–43]. These kind of
87 approaches have been used on 600K Affymetrix® Axiom® SNP array to detect several hundreds of CNVs
88 and to explore the contribution of CNV to phenotypic variation [44].

89 With the emergence of massive parallel sequencing, new methods have been developed to detect
90 structural variations based on the alignment of resequencing reads onto a high quality reference genome
91 sequence. Among these, three have been mainly used [45] : (i) the “read-depth” (RD) method, which can
92 only detect copy number variations; (ii) the “read-pair” (RP) method, which can detect deletions as well
93 as small insertions (up to the size of the library insert); and (iii) the “split-read” (SR) method which can
94 also detect deletions and small insertions (up to the size of a read). Chia et al. (2012) used the RD approach
95 to identify CNVs among 104 maize lines and performed association studies for several traits [10].
96 However, the RD method does not allow the identification of novel sequences and is error prone,
97 especially regarding the size of the discovered CNVs which greatly depends on the size of the sliding
98 window used. The RP method has been implemented in many computational tools like BreakDancer [46]
99 and has been widely used. Although it has proven to be highly efficient to detect deletions [47–49], this
100 approach suffers from two limitations: it does not allow precise detection of breakpoints, and the size of
101 the insertions which can be detected is directly limited by the library insert size. The SR method, which
102 was first implemented in PInDel [50], has the advantage of defining breakpoints at a single-base
103 resolution, but again the size of the detectable inserted sequence is limited.

104 The “assembly” (AS) method is able to detect all types of SVs of any size, but is also the most cost
105 and computation-intensive. It is the only method able to detect large insertions with precise breakpoint
106 definition. However, the assembly of large and complex genomes such as maize remains very expensive
107 and computationally intensive, despite recent progress in this area [20, 21, 31]. There has been in the past
108 some attempts to reduce this complexity by reducing the number of sequences to assemble. For instance,
109 Lai et al., (2010) identified 104 deletions and 570 insertions among 6 maize inbred lines by assembling
110 genomic regions from reads that did not map on the B73 reference genome [51]. The sequences
111 assembled by this approach were enriched in erroneous reads or reads coming from external
112 contamination, and they were too short to be anchored to the reference genome B73. Hirsch et al. (2014)
113 identified several putatively expressed genes that were not present within B73 reference genome by
114 assembling and comparing the transcriptome of hundreds of inbred lines [12]. This new approach was
115 limited to the transcribed part of the genome and suffered from a high level of false positives. More
116 recently, Lu et al., (2015) used genotyping by sequencing approaches on 14,129 inbred lines to identify
117 1.1 million short and unique sequences (GBS tags) that (i) did not align on the B73 reference genome, or
118 were aligned but outside of a 10Mbp windows around their mapped position; or (ii) were mapped at the
119 same location by joint linkage mapping in NAM populations using co-segregation with a SNP and logistic
120 regression between the InDel and the SNP in an association panel [13]. The main drawback of this
121 approach is the high percentage of missing data due to the low depth of sequencing, which requires
122 imputation before being able to perform genetic analysis. Recent whole genome sequence assemblies of
123 PH207 [31], and F2 [20] have allowed the identification of thousands of large InDel and PAV sequences.
124 For instance, 2,500 genes were found either present or absent in PH207 and B73 genomes and 10,735
125 PAV sequences larger than 1kb were discovered between F2 and B73, including 417 novel genes in F2.
126 These discovery approaches have been limited to a few individuals due to sequencing costs and
127 computational challenges, so they have not been adapted for characterization of SVs on large maize
128 panels. Darracq et al. (2018) developed an interesting approach for the genotyping of PAVs from mapping
129 of low depth (5-20X) resequencing datasets [20]. This method is based on the comparison of reads aligning

130 to the region found in F2 and in the line of interest. While this method is potentially adapted to genotype
131 PAVs on any set of line with low resequencing data, it has been so far used for PAV genotyping on a low
132 (<30) number of maize lines. Moreover, it is restricted to the analysis of PAVs, and is not adapted for
133 genotyping other types of SVs. To avoid this ascertainment bias due to use of a single reference genome
134 to genotype SV, other studies proposed to call SV by aligning reads on a pan-genome representing the
135 combination of several genomes [14, 22, 52]. However, these approaches remained computationally
136 challenging on a sizable set of individuals, time demanding, and costly for large and complex genomes,
137 since it requires high-depth sequencing [52]. To our knowledge, no high-throughput genotyping approach
138 has been developed for genotyping large numbers of InDels, including PAVs, on a large set of individuals.
139 We have developed, as proof of concept, a new high-throughput and affordable array that is able to
140 genotype simultaneously large insertions and deletions, with highly variable size and contents that are
141 previously discovered by different sequencing methods. In this study, we present this approach which is
142 both (i) comprehensive, as it includes the discovery and localization of deletions as well as insertions
143 regarding the B73 reference genome at the base pair level and (ii) high-throughput, as it allows genotyping
144 of thousands of InDels on hundreds of individuals. Our strategy takes advantage of next generation
145 sequencing (NGS) technologies and recent advances in assembly of complex genomes. It also benefits
146 from the high efficiency of SNP arrays like the high-throughput Affymetrix® Axiom® technology. In this
147 paper, we detail how we discovered thousands of small to large InDels, including PAVs, from three maize
148 inbred lines (F2, PH207 and C103) as compared to the B73 reference genome. We then describe how we
149 designed and selected 600,000 probes to create a new Maize Affymetrix® Axiom® array to genotype these
150 InDels. Finally, we describe how we successfully used this array to genotype an association panel of 362
151 maize inbred lines.

152 Results

153 InDel and PAV discovery

154 To design a comprehensive InDel genotyping array, we first discovered a set of InDels which would
155 be representative of the maize temperate germplasm. We already had access to sequence data for the
156 European flint line F2, and we benefited from a first set of 42,330 F2-specific sequences, larger than 150pb
157 and totaling 16Mbp. This dataset was derived from the *de novo* assembly of an F2 paired-end that failed
158 (at least for one read of the pair) to align onto the B73 AGPv2 sequence, and which were totally devoid of
159 coverage by B73 reads (“Reference guided assembly” in Additional file 2: Figure S1, “no map” approach).
160 We also took advantage of the work done by [20] to add another 10,044 F2-insertions (size >1 kb, total
161 size of 88Mb), with less than 70% of their length covered by B73 reads discovered by a whole genome
162 assembly approach (Additional file 2: Figure S1).

163 To complement these two datasets of F2/B73 deletions and insertions, we generated and
164 assembled Illumina® paired-end and mate-pair sequences from two other key founders of temperate
165 maize breeding programs: PH207 and C103. We then used this F2, PH207, and C103 sequence data to
166 detect all InDels, including PAVs, at base-pair resolution, between these three lines and B73. As opposed
167 to the “reference guided assembly approach”, the “whole genome assembly” methodology allowed us to
168 access both to their sequences and their breakpoints, permitting the genotyping of such InDels in several
169 individuals (more details in Methods). We did not use the “no map” approach for InDel discovery on
170 PH207 and C103, because this approach did not give access to breakpoint resolution, did not allow the
171 discovery of InDels without knowledge of the specific sequence, and was almost redundant with the
172 assembly approach.

173 We first aligned F2, PH207, and C103 sequences against the B73 reference genome sequence in
174 order to detect deletions. Here, the term “deletion” does not reflect any underlying biological process of
175 DNA excision but refers to a sequence of at least 100bp present in the B73 genome at one locus and
176 absent in another line at the same locus. Deletions were detected for the three lines simultaneously using
177 the “genotyping” option of PInDel [50], generating a set of 26,368 non-redundant deletions with precise
178 identification of their breakpoints (Additional file 2: Figure S2A). The number of deletions found for each
179 line was similar, respectively 12,165, 11,922, and 13,432 for F2, PH207, and C103. 67% of the deletions
180 found were unique to one line, 24% were shared by two lines, and 9% by three lines (Additional file 2:
181 Figure S2A). These results confirm the good complementarity of the lines chosen to discover InDels. The
182 high proportion of unique deletions among 4 lines may also reflect that numerous InDels remain to be
183 discovered in temperate maize germplasm.

184 Next, we generated a draft genome assembly for each of these lines, which was used as a
185 template for alignment of B73 reads to detect insertions relative to the B73 reference genome (Additional
186 file 1: Table S1). As for deletions, here the term “insertion” does not reflect any underlying biological
187 process of DNA integration, but defines a sequence larger than 100bp that is present in one line at a given
188 locus, and absent from B73 at the same locus. These three draft assemblies cover less than one third of

189 the expected maize genome size but include a large portion of low copy sequences, including genes, as
190 shown by BUSCO results (Table 1).

Table 1: F2, PH207, and C103 de novo assembly metrics.

Maize line	Number of scaffolds	Min size	Max size	Average size	N50	Total (Mb)	% of Ns	Complete BUSCOs (C)	Fragmented BUSCOs (F)	Missing BUSCOs (M)
F2	76,563	892	112,956	16,900	14,04	646.3	9.48%	89.3%	4.9%	5.8%
PH207	81,688	884	2,024,489	29,557	16,86	797.5	8.90%	91.8%	2.7%	5.5%
C103	84,990	886	120,582	19,305	16,14	793	8.21%	90.6%	4.2%	5.2%

Number of scaffold: The number of scaffold sequences assembled, Min Size: the length of the shortest scaffold, Max size: the length of the longest scaffold, Average Size: the average size of scaffolds, N50: N50 of the assembly, Total: the total number of bases included in the assembly, % of Ns: the percentage of Ns present in the assembly; BUSCO statistics included the percentage of complete (C), fragmented (F) and missing (M) BUSCO genes from a total of 1440 BUSCO genes

191 Detection of insertions was processed separately for each inbred line and generated 28,221 insertions for
192 F2, 27,904 insertions for C103, and 26,795 insertions for PH207, with their precise breakpoints (Additional
193 file 2: Figure S2B). The number of insertions is similar between lines, but significantly greater than the
194 observed deletions. Among these insertions, 26,691 cases could be uniquely anchored at base pair
195 resolution onto the B73 reference genome sequence (Additional file 2: Figure S2B). Again, a majority of
196 insertions were unique to one line (72%) confirming the complementarity of the material chosen (Figure
197 S2B).

198 Finally, the results from the different approaches were merged into a non-redundant set of
199 141,325 InDel sequences (see Methods), comprising 52,175 deletions and 89,150 insertions. These
200 regions were then used for the design of genotyping probes.

201 Design of the genotyping array

202 Genotyping strategy

203 Large InDels can be efficiently genotyped with a SNP array using a combination of two types of
204 probes: (i) “external” probes, which target breakpoints using the two flanking sequences of a given InDel
205 (BP probes), and (ii) “internal” probes, which target presence/absence regions (PARs) within the internal
206 sequence of InDels on polymorphic (OTV probes) or monomorphic sites (MONO probes). We define PARs
207 as small portions of DNA sequence of at least 35bp that were observed present or absent at the genome
208 level, when comparing two individuals. They are thus suitable for the design of presence/absence

209 genotyping probes. Ideally, each InDel should be called by two BP probes on either side and by multiple
210 internal probes, regularly distributed along the internal sequence of the InDel (Figure 1A). However, in
211 practice, this combination of different probes is not always possible. For instance, precise breakpoints
212 were not determined for all PAVs from our “no map” approach and [20], and PARs for internal probes
213 were not always found in our InDels.

214 **Probe design**

215 BP probes should behave like classical SNP probes where one allele corresponds to the presence
216 and the other to the absence of the InDel. They are useful to explore the conservation of the localization
217 of large insertion/deletion events across multiple individuals, even when no internal probe can be
218 designed due to the absence of PARs. Among the 141,325 selected variants, 86,406 InDels (22,420
219 deletions and 63,986 insertions as compared to the B73 reference genome sequence) had breakpoints
220 defined at base-pair resolution and were suitable for BP probe design. Four different breakpoint types
221 were identified according to the presence of micro-homology and/or shorter non homologous sequence
222 [53] in place of a complete deleted sequence (Additional file 2: Figure S3): (type I) 3,397 cases with sharp
223 breakpoints; (type II) 45,987 cases with a micro-homology sequence (8.6 bp on average and no more than
224 237 bp) which was present in one copy in the reference sequence and duplicated at both extremities of
225 the novel inserted sequence; (type III) 36,893 cases harboring insertion of a short non-homologous
226 fragment (42.2 bp on average and up to 892 bp) in place of a large deleted sequence; and (type IV) 156
227 cases with a combination of type II and type III breakpoints. Following Affymetrix® recommendations,
228 19,010 InDels with type II breakpoints having a micro-homology sequence longer than 5bp were excluded
229 from the design process. In the end, 67,396 InDels, representing 48% of all available InDel variants, were
230 submitted to the Affymetrix® design pipeline. Two probes, one on forward (FW) and one on reverse (REV)
231 strand, were designed for each breakpoint. These probes were classified as *not possible* (18%), *not*
232 *recommended* (33%), *neutral* (15%) and *recommended* (35%) by this automated pipeline (see Methods
233 for details), leaving 33,430 InDels (51%) that could be targeted by at least one *recommended* probe.

234 Internal probes, which should behave like “off-target” variants [36] where the hybridization of the
235 probe indicates presence of the InDel, and the absence of hybridization of the probe indicates absence of
236 the InDel, are useful to explore the genetic diversity within InDel sequences (Figure 1 D). They will also be
237 particularly interesting to target InDels for which no breakpoint could be identified (such as PAVs from
238 the “no map” approach).

239 For the design of OTV probes, we benefited from the availability of SNPs which had been
240 previously identified from the alignment of resequencing data from a core collection of 25 temperate
241 maize inbred lines against the B73-F2 maize pan-genome from [20]. As a consequence, OTV probes have
242 only been designed for deletions positioned on the B73 reference genome and F2 insertions coming from
243 [20]. Among these, the context sequences of 436,162 SNPs, corresponding to 21,390 InDels, were
244 extracted and submitted to the Affymetrix® design pipeline. Two probes, one on forward (FW) and one
245 on reverse (REV) strand, were designed for each SNP. A total of 872,324 OTV probes could be designed
246 and scored as *not possible* (0.05%), *not recommended* (71%), *neutral* (14%) and *recommended* (16%),
247 leaving 17,589 InDels (82%) which could be targeted by at least one *recommended* probe.

248 For the design of BP and OTV probes we could rely on Affymetrix® design pipeline to identify
249 probes localized in PARs and thus suitable for the Affymetrix® Axiom® technology. For the design of MONO
250 probes, we first had to identify such PARs within 141,325 InDels cumulating 133Mbp of sequence. We
251 used sequence masking methods to exclude repeats based on similarity to known maize repeats or on
252 occurrence of 17-mers found within the sequencing datasets we had for B73, F2, PH207, and C103 (see
253 Methods). By doing so, we identified 122,972 PARs, representing a cumulated size of 27Mbp,
254 corresponding to 20.3% of the initial size and allowing the possibility to design MONO probes for 79,987
255 InDels (56.5%). These PAR sequences were successfully used for the design of 25,735,797 MONO probes,
256 among which 59% were scored as *recommended* and allowed to target 62,875 InDels (79%).

257 With this combined approach, we designed a total of 26,715,361 probes targeting 117,756 InDels,
258 which represent a cumulated length of 250 Mbp including 27 Mbp of PARs (Table 2).

Table 2: Number of probes and targeted InDels before and after selection for array design and passing the Affymetrix® quality control according to different probes type. Percentages are indicated in brackets

	Before selection		On array		Called by Affymetrix® pipeline	
	Probes	InDel ⁺	Probes	InDel ⁺	Probes	InDel ⁺
BP Type1	6,648 (0.02%)	3,324 (2.82%)	4,691 (0.71%)	2,751 (2.6%)	2,092 (0.44%)	1,482 (1.66%)
BP Type2	51,770 (0.2%)	25,885 (21.98%)	38,790 (5.85%)	22,662 (21.39%)	20,540 (4.29%)	14,407 (16.12%)
BP Type3	71,820 (0.27%)	35,910 (30.5%)	41,272 (6.23%)	27,897 (26.34%)	23,631 (4.93%)	18,485 (20.68%)
BP Type4	312 (0.001%)	156 (0.13%)	241 (0.04%)	146 (0.14%)	119 (0.02%)	93 (0.1%)
OTV	872,324 (3.26%)	21,390 (18.16%)	163,278 (24.64%)	18,558 (17.52%)	96,867 (20.22%)	15,064 (16.85%)
MONO	25,735,797 (96.25%)	68,573 (58.23%)	414,500 (62.54%)	65,796 (62.11%)	335,778 (70.1%)	63,597 (71.14%)
ALL	26,738,671	117,756	662,772	105,927	479,027	89,393

^{*}Note that a same InDel could be genotyped by several probe types which resulted in the percentage values great than 1.

259 Among these InDels, 97,748 (83%) can only be targeted with either internal or external probes, but not
260 both (Figure 3A). These results support our overall strategy which includes the discovery of InDels, with
261 precise breakpoints in a preliminary step, and the use of complementary internal/external probes for the
262 genotyping of large InDels.

263 **Array design**

264 We used the Affymetrix® recommendations to select the 700,000 probes to be included in the
265 final array, plus some other criteria depending on the probe type. Nevertheless, because of their added
266 value, we decided to keep all BP probes as long as they had less than 3 hits on the B73 reference genome
267 sequence. This first selection consumed 84,994 probes targeting 53,456 InDels, among which 70% could
268 only be targeted by BP probes. Concerning OTV and MONO probes, we first selected *neutral* and
269 *recommended* probes having no hit at all (for insertions), and only one hit (for deletions), against the B73
270 reference genome sequence. We then considered their density with the objective to maximize the
271 number of InDels that could be surveyed, as well as to have an even distribution of probes along targeted
272 InDel sequences (see Methods). We then performed a second selection among *not recommended* OTV
273 and MONO probes for 4,541 InDels that were still not targeted. After filtering some duplicated probes,
274 we built a final array design containing 662,772 probes targeting 105,927 InDels that represent a
275 cumulated length of 232 Mbp, including 25.9 Mbp of PARs.

276 **Description of the array content**

277 The final array design allows genotyping InDels with various sizes, ranging from 37 bp to 129.7
278 kbp, with a median of 501 bp (Figure 2). They are covered by 1 to 482 probes, with a median of 3 probes
279 per InDel (Additional file 2: Figure S4). The number of probes does not always reflect the length of the
280 InDels, as the proportion of PARs within InDels is highly variable (Figure 2A). 8,040 InDels (ranging from
281 37 bp to 2,409 bp, with a median of 163 bp) were completely covered by PARs and could thus be
282 considered as a proper PAVs, 34,372 InDels (ranging from 101 to 129,700 bp with a median of 320 bp)
283 were not covered by any PAR at all (Figure 2A). The biggest InDels contains more frequently PARs than
284 the little ones (Figure 2B). In fact, the number of internal probes were more strongly correlated to the size
285 of the PARs ($r^2 = 0.79$) rather than to the size of the InDels ($r^2 = 0.16$) (Additional file 2: Figure S5).

286 As expected, the probe selection process did not impact the overall distribution of probe types
287 among targeted InDels, as 35% of them can exclusively be genotyped by BP probes, and 50% can only be
288 genotyped by internal probes, among which 73% are only targeted by the use of the original MONO
289 probes (Figure 3B). Indeed, a large number of InDels did not contain PARs and cannot be genotyped with
290 35bp internal probes but only with BP probes. Whereas, others InDels contains PARs but have no BP
291 probes due to the InDel discovery approach (“no map”).

292 Among the 43,117 InDels that could be anchored onto the B73 reference genome sequence and
293 which were included in the array design, 13,737 were located inside a gene, 57 close to a gene (less than
294 1 kb away), 1,311 inside a pseudo-gene and 2,212 inside a transposable element. InDels and probe density
295 varied across each chromosome (Additional file 2: Figure S6). We observed a higher density in
296 chromosome arms than in peri-centromeric regions (Additional file 2: Figure S6). We also identified
297 clusters of InDels with a large specific sequence at the beginning of chromosome 6 (10-20Mbp) or at the
298 end of chromosome 5 (~190Mbp).

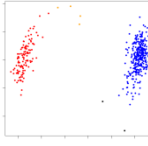
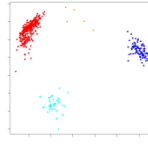
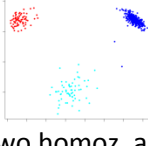
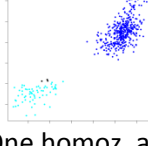
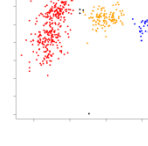
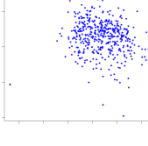
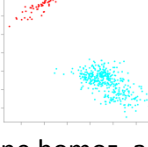
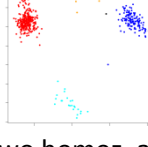
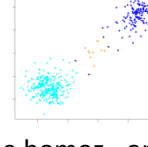
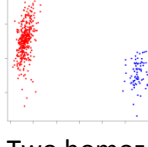
299 **Assessing array quality by genotyping 105,927 InDels on** 300 **480 maize DNA samples**

301 **InDel calling using dedicated Affymetrix® pipelines**

302 We genotyped 480 maize DNA samples including 440 inbred lines, 24 highly recombinant inbred
303 lines and 16 F1 hybrids. Dedicated Affymetrix® pipelines were implemented for each of the probe types
304 to call genotype of the InDels based on fluorescent intensity and contrast variation of the probes. It
305 included two algorithms already developed by Affymetrix® [36] for BP and OTV probes (Additional file 2:
306 Figure S7A et B) and a third one, which was newly developed for the calling of presence/absence
307 genotypes using MONO probes (Additional file 2: Figure S7C). 35 DNA samples including all F1 hybrids, did
308 not pass Affymetrix® quality control due to their low call rate (<0.9) and were eliminated. Call rate of the
309 445 remaining samples, which are all inbred lines, varied from 96% to 99% with a median of 98%. The call
310 rate varied according to probe type (median of 90% and 99% for BP and internal probes, respectively).
311 Out of 662,772 probes, 479,027 probes representing 89,393 InDels passed Affymetrix® quality control and
312 were called on 445 DNA samples. Respectively 55%, 59%, and 81% of BP, OTV, and MONO probes were
313 converted into recommended markers after clustering by Affymetrix® pipelines (Additional file 1: Table
314 S2, S3, and S4). 94% of these recommended BP and OTV markers were classified as “PolyHighResolution”
315 (PHR) indicating a high quality of clustering and that these markers were polymorphic (Additional file 2:
316 Figure S8). Note that the criteria defining high quality of clustering for MONO probes called by new
317 Hom2OTV algorithm was not yet implemented in Affymetrix pipeline (Additional file 1: Table S4 and
318 Additional file 2: Figure S7C). As a consequence, classification of MONO probes could not be comparable
319 to BP and OTV probes. Thanks to the 3 probe types and redundancy, 84% of all InDels could be called with
320 an average of 5.4 probes per InDel.

321 To evaluate the genotyping ability of the 479,027 probes, we first compared the clustering of
322 inbred lines expected for three probe types (BP, OTV, and MONO) with the observed clustering of inbred
323 lines based on fluorescence intensity and contrast of 445 inbred lines genotyped with the array. For BP
324 probes, we expected at least two clusters corresponding to the individuals homozygous either for
325 presence (“AA” or “BB”) or absence (“OO”). A third cluster could be observed when individuals were
326 heterozygous individuals for presence/absence (“OA” or “OB” hemizygous) (Figure 1C). For OTV probes,
327 we expected at least 3 different clusters: two cluster corresponding to the individuals homozygous for
328 allele A or B of SNP (“AA”, “BB”), and a third “off-target” cluster for the individuals homozygous for
329 absence (“OO”). A fourth cluster could be observed when some individuals were heterozygous at the
330 within-InDel SNPs (AB). For MONO probes, we expected only two clusters corresponding to the individuals
331 for which the sequence was present (“AA” or “BB”) or absent (“OO”, “AA” or “BB”) (Figure 1C). The
332 observed clustering by the three dedicated pipelines was consistent with the expected clustering for 43%
333 of BP, 83% of OTV and 63% of MONO probes (Table 3).

Table 3: Comparison between the clustering expected for BP, MONO, and OTV probe types and the clustering produced by Affymetrix® pipelines based on the fluorescent intensity and contrast of 445 inbred lines for 479,027 probes.

		Classification based on the clustering produced by Affymetrix® pipelines and genotyping assignment			
Probe types		BP	OTV	SNP	monomorphic
BP	Number (%)	20,370 (43.9%)	26,012 (56.1%)		
	Clustering examples				
	Description	Two homoz. clusters	Two homoz. and one OT clusters		
OTV	Number (%)	78,799 (81.3%)	502 (0.5%)	17,562 (18.1%)	4 (0.0%)
	Clustering examples				
	Description	Two homoz. and one OT clusters	One homoz. and one OT clusters	Two homoz. clusters	One cluster
MONO	Number (%)	212,434 (63,3%)	15,690 (4,7%)	68,562 (20,4%)	1,981 (0,6%)
	Clustering examples				
	Description	One homoz. and one OT clusters	Two homoz. and one OT clusters	One homoz., one OT and one het. clusters	Two homoz. clusters

“Clustering example”: typical example of clustering based on the fluorescent intensity (y-axis) and contrast (x-axis). Colors on figure indicate the assignation of the genotype to the individuals based on this clustering; “Number (%)"": Number (percentage) of probes displaying the corresponding clustering. “Description”: Brief characteristic of each classification based on the clustering of individuals (homoz.= homozygote, het=heterozygous, OT= off-target).

334 We observed also some unexpected clustering. For 57% of BP probes, we observed an additional
335 off-target cluster (OTV in Table 3). This indicates that some BP probes did not hybridize properly in some
336 inbred lines, which can either be due to the presence of polymorphism within flanking sequences of the
337 targeted InDels or to the existence of more complex rearrangements removing the breakpoints.

338 Regarding MONO probes, 25% displayed additional cluster(s) when the sequence was present
339 suggesting the presence of single nucleotide polymorphisms at this position. Among these, we were able
340 to distinguish two types of clustering (Table 3). 4.7% of MONO probes exhibited a clustering similar to
341 those observed for OTV probes suggesting that these MONO probes revealed, by chance, a single
342 nucleotide polymorphism. In contrast, 20.4% of MONO probes displayed an unexpected clustering pattern
343 for inbred lines with the presence of a heterozygous cluster but absence of a second homozygous cluster
344 for SNP (Additional file 2: Figure S9B). In the end, 2.8% of MONO probes displayed an additional
345 heterozygous cluster for SNP when the sequence is present but no “off target” cluster corresponding to
346 individuals for which the sequence is absent (Additional file 2: Figure S9D).

347 For 18% of OTV (Additional file 2: Figure S9A) and 8.3% of MONO probes, clustering displayed no
348 “off target” cluster for absence, suggesting no presence/absence polymorphism at this position (Table 3).
349 Note that some BP were also classified as monomorphic for presence/absence but were filtered out by
350 the BP pipeline (“MonoHighResolution” in Additional file 1: Table S2 and Additional file 2: Figure S8). These
351 monomorphic probes originated from false positive discovery of InDels or PARs within InDels that are not
352 present/absent elsewhere in the genome of four lines (see Discussion). After removing these
353 monomorphic probes for presence/absence, 422,369 probes allowed us to successfully genotype a total
354 of 86,648 InDels (82% of 105,927 InDels targeted by the array) on 445 inbred lines.

355 **Evaluation of genotyping reproducibility and quality**

356 ***Consistency of genotyping among the four inbred lines used for InDel discovery***

357 We used the 479,027 probes passing Affymetrix® quality controls to evaluate the quality of
358 Presence/Absence genotyping by comparing the genotyping results obtained from our array (GBA:
359 Genotyping By Array) with those from sequencing (GBS: Genotyping by Sequencing) for the 4 lines used
360 for the discovery of InDels (B73, F2, PH207, and C103). Respectively, 97%, 912%, and 88% of the BP, OTV,
361 and MONO probes had a genotyping result consistent with results obtained from BLAST alignments
362 against our three draft genome assemblies and the B73 reference genome. We observed a strong
363 asymmetry for concordance rates for internal probes (OTV and MONO) depending on whether the
364 genotype has been called by sequencing as present or absent (95% vs 80% present and absent,
365 respectively, Table 4). Interestingly, we observed no asymmetry for BP probes that are designed
366 exclusively on B73 genome compared to OTV and MONO probes that are designed from the 4 genome
367 assemblies (Table 4). These low consistencies for internal probes when genotype by sequencing indicated
368 absence could be explained by the use of incompletely assembled genomes of the three lines (PH207,
369 C103, F2) to call the presence/absence genotype from sequencing.

Table 4: Consistency rate between genotyping by sequencing and by array for the 4 individuals used to discover the InDels, for the three probe types and for the two different genotypes observed from sequencing: presence (P) or absence (A).

Probe Types	Genotype by sequencing	B73	F2	C103	PH207	All Lines
BP	A	0,98	0,98	0,98	0,97	0,98
	P	0,97	0,97	0,97	0,96	0,97
	ALL	0,97	0,97	0,97	0,97	0,97
OTV	A	0,85	0,89	0,80	0,78	0,83
	P	0,93	0,97	0,96	0,96	0,96
	ALL	0,90	0,95	0,91	0,90	0,92
MONO	A	0,77	0,81	0,82	0,81	0,80
	P	0,90	0,98	0,94	0,94	0,95
	ALL	0,82	0,94	0,89	0,88	0,88
ALL	A	0,80	0,86	0,84	0,82	0,82
	P	0,92	0,97	0,94	0,95	0,95
	ALL	0,85	0,95	0,90	0,89	0,90

*Note that consistency rate of hemizygous genotypes (heterozygous for presence / absence) were not displayed in the table for BP probes but considered to estimate global consistency rate (ALL). Note that the absence of probe sequence due to absence of hybridization or no alignment on draft sequence of BP probes were considered as missing data. Missing data were not included in the comparison for all probes.

370 If the genomic region containing the InDels were absent or badly assembled in at least one line, some
 371 probes would not align properly, resulting in false absence calls, instead of presence in GBS. The four
 372 inbred lines showed very similar concordance rates, F2 being the most concordant (95%). This could be
 373 partially explained by the higher proportion of GBS present calls in F2 as compared to the three other lines
 374 since GBS present calls are more consistent with GBA than GBS absent calls. The median consistency rate
 375 of probes within InDels remained relatively high and stable, around 90%, independently of the number of
 376 probes per InDel (Figure S10), suggesting no relationship between the consistency rate of individual
 377 probes and length of PARs within InDels.

378 ***Consistency among probes from the same InDel***

379 To estimate the consistency of different probes for typing a given InDel, we analyzed genotyping
 380 results for 50,648 InDels genotyped with at least two probes in a collection of 362 temperate inbred lines.
 381 For each InDel and each inbred line, we calculated the average allelic frequency of presence over all
 382 probes. Frequencies of 1 (presence) and 0 (absence) indicated that all probes displayed consistent
 383 genotyping for the corresponding inbred line (Figure 1D and Figure S11A). Alternatively, frequencies
 384 different from 0 or 1 (FreqDiff01) indicated that at least one probe displayed inconsistent genotyping with
 385 other probes for corresponding inbred lines (Figure S11B). Overall, 75% of the InDel genotyping resulted
 386 in an average allelic frequency for the presence of 1 or 0, meaning that all probes had a consistent
 387 genotyping results for calling the allele at both present or absent states, respectively (Figure 4A).

388 However, we observed a strong variation of median (average) allelic frequency difference from 0
 389 or 1 (FreqDiff01), according to the number of probe interrogating that InDel (Figure 4B, Additional file 1:
 390 Table S5). Median (average) FreqDiff01 across InDels varied from of 1.2% (9.8%) to 58% (52%) when the

391 number of probes varied from 0 to 30 (Figure 4B, Additional file 1: Table S5). We compared this variation
392 to what could be expected for different probe genotyping error rates (1%, 3%, 5%, and 10%). Based on
393 this comparison, we estimated the probe genotyping error rate is approximately 3% (Figure 4). For InDels
394 with fewer probes (<10), the average and median FreqDiff01 differed slightly, suggesting that some InDels
395 with low probe numbers displayed high genotyping inconsistencies among their probes (Figure 4,
396 Additional file 1: Table S5). In order to evaluate whether probe genotyping error is similar for present or
397 absent calls, we analyzed the variation of FreqDiff01 with regard to the average frequency of absence of
398 InDel sequences in 362 lines (Additional file 2: Figure S12A). The median FreqDiff01 was higher for InDels
399 which have their sequence more frequently absent than present across 362 lines, regardless of the
400 number of probes (Additional file 2: Figure S12B). It suggested that genotyping was more accurate for
401 absence than presence. This was logical, considering that polymorphisms within probes would preclude
402 hybridization of the probes for some lines, and it would result in absent calls with MONO and OTV probes,
403 while polymorphisms within probes have no impact when the sequences are absent.

404 Combining genotyping from multiple probes within InDels greatly improved reliability of InDel
405 genotyping, since it allowed (i) to correct the individual genotyping errors due to polymorphisms within
406 probe sequences, (ii) to reduce the missing data rate due to bad clustering or probes polymorphisms, and
407 (iii) to remove probes displaying highly-divergent genotypes compared to other probes for the same InDel,
408 due, for example, to a bad design of the probes. In order to evaluate the combining of genotypes of several
409 probes on the accuracy of InDel genotyping, we simulated global genotyping error rates for InDels by
410 assigning to each inbred line the most frequent allele, based on the average frequency over all probes
411 from an InDel, with various genotyping error rates (Additional file 1: Table S6). By this approach, the
412 genotyping error for InDels was greatly reduced. Considering a probe genotyping error of 5%, the
413 genotyping error of InDels for inbred lines were reduced to 0.2% and 0.1%, when the number of probes
414 within the InDels were 2 and 5, respectively (Additional file 1: Table S6). Combining genotypes from
415 several probes also strongly reduced the average missing data rate for InDels; it decreased from 2.3% to
416 0.2%, when the number of probes increased from 2 to 5 (Additional file 1: Table S5). However, some
417 contradictory probe genotypes were repeatedly found across the 362 samples (Additional file 2: Figure
418 S11B), suggesting that some probe inconsistencies could have biological origins (*i.e* more complex
419 rearrangement), rather than being genotyping errors. Additionally, 35% of InDels called by BP had their
420 FW and REV probes classified differently (e.g. one as BP and the other as OTV). Altogether, these results
421 suggest that some calling inconsistencies between probes within InDels could come from polymorphisms
422 in the flanking sequence while some other could be due to local rearrangements in the genotyped lines
423 as compared to the lines used for InDels discovery.

424 ***Reproducibility and Mendelian inheritance***

425 Genotyping reproducibility was evaluated by comparing genotypes between five DNA replicates
426 corresponding to unique F1 hybrids derived from a cross between B73 and F72 for all probes type. Median
427 reproducibility was 95%, 96%, and 97% for BP, OTV and MONO probes respectively. Interestingly, there is
428 some variation of reproducibility relative to probe clustering (Additional file 1: Table S7). Note that
429 Affymetrix[®] algorithms were not specified to genotype hemizygote using OTV and MONO probes in this
430 dataset. We also performed a parent-offspring analysis on 12 F1 hybrids derived from 9 parental lines by

431 comparing genotypes observed of these F1 hybrids with those predicted from genotypes of their two
432 parental lines for 46,382 BP probes (Additional file 1: Table S8). On average, 95% and 77% of observed
433 genotypes were consistent with those predicted from parental lines for homozygous and hemizygous
434 genotypes, respectively (Additional file 1: Table S8). The consistency rate was slightly higher when
435 genotypes were absent (98%) than present (94.5%). Note that the seed-lot of parental lines used for
436 producing F1 hybrids were different from those genotyped, which could explain lower consistencies rate
437 than for DNA replicate of F1 hybrids. Note also that the genotypes of all F1 hybrids have been initially
438 eliminated by Affymetrix® quality control due to their low call rate and were therefore forced for
439 reproducibility analysis. This low call rates can be attributed to the fact that these samples had different
440 genotype cluster properties (probe intensity profiles) compared to the samples that passed QC. As a
441 consequence, this strongly increased the missing data rate for the F1 hybrids for OTV and MONO probes.

442 In the end, we evaluated genotyping reproducibility for inbred lines, by comparing the genotyping
443 results of 13 different inbred lines that were replicated in the experiment (Additional file 1: Table S9).
444 Note that these are not perfect biological replicates, as they represent the same variety but come either
445 from different seed lots or from different accessions. These replicates exhibited a genotyping difference
446 varying from 0.6% to 5.2% (Median = 1.7%, Additional file 1: Table S9). This is similar to the amount of
447 inconsistencies obtained on the same material using a 50K SNP array [54], suggesting that InDel
448 genotyping inconsistencies for replicates can be attributed mostly to seed-lot divergences, rather than
449 genotyping errors (Additional file 1: Table S9). However, genotyping reproducibility was higher for these
450 inbred lines than for the DNA replicates of the F1 hybrid, suggesting that errors in F1 hybrids can mostly
451 be attributed to the inability to genotype hemizygous with OTV and MONO probe for this small dataset.

452

453 **Application: Diversity analysis of 362 maize inbred lines 454 panel**

455 In order to evaluate this new array for genetic analysis, we analyzed genetic diversity using 57,824
456 polymorphic InDels on a subset of 362 inbred lines, representing genetic variation that has been
457 successfully used to decipher maize genetic structuration and perform genome-wide association studies
458 [55–57]. To represent each InDel in the diversity analysis, we selected one single probe per InDel, based
459 on the probe genotyping quality (see Methods).

460 We first compared kinship values between 362 inbred lines estimated with 57,824 InDels and with
461 28,143 prefixed Panzea SNPs from the 50K SNP array. Kinship values between lines obtained with SNPs
462 and InDels were strongly similar and highly correlated ($r=0.9$), except those for a couple of lines closely
463 related to B73 and F2 (Additional file 2: Figure S13). Then, we performed Principal Coordinate Analysis
464 (PCoA) based on the genetic distance between 362 lines estimated by InDels and SNPs (Figure 5). We
465 included on this PCoA the genetic structuration of these 362 inbred lines, as obtained from the prefixed
466 Panzea SNPs from the 50K SNP array [55]. The global genetic structure developed using two types of
467 polymorphisms are highly similar. The first axis showed good discrimination of European Flint from Corn
468 Belt Dent and Stiff Stalk lines, while the second axis discriminated European Flint and Northern Flint lines.

469 Overall, the clustering of individuals based on genetic distance estimated with InDels (Figure 5A) was
470 consistent with those estimated with SNPs (Figure 5B). We observed that B73 and F2, which were used to
471 discover the majority of InDels, were more contrasted on PCoA when genetic distance was estimated with
472 InDels, as compared with SNPs from the 50K array, indicating some ascertainment bias. We thus
473 performed two PCoAs, with InDels and SNPs, excluding B73 and F2 (Additional file 2: Figure S14). The two
474 PCoAs gave similar patterns, suggesting that this ascertainment bias was largely removed when no close
475 relative lines from those used for discovering InDels were used in diversity analysis. Due to this
476 ascertainment bias, result of our array should be therefore interpreted with caution for diversity analysis.

477 Discussion

478 1. An original high throughput approach for 479 genotyping InDels

480 The comparison of whole genome sequence assemblies is in theory the best approach to identify,
481 precisely and exhaustively, structural variations between two individuals. But even though great progress
482 has been made recently in this area, high-quality, whole genome assembly is still too costly, time-
483 consuming, and computationally intensive to be applied to hundreds of individuals, especially when
484 considering the complexity of the maize genome [20, 58]. Other whole genome sequencing approaches
485 based on alignment of reads on a single reference, and using either “read-depth”, “read-pair”, or “split-
486 read” identification methods [46–50] have mostly been limited to the identification of deletions (i.e.
487 sequences absent from a reference genome). Liu et al., (2015) partially addressed the lack of insertions
488 (i.e. novel sequences compared to a reference genome) by the identification 1,973,746 InDels [4].
489 Although, among these a majority were very small (85% smaller than 11bp), and the use of PCR markers
490 to genotype them is time-demanding, labor-intensive, and costly at a large-scale level. To avoid this
491 ascertainment bias due to use of a single reference genome to genotype SVs, other studies proposed to
492 call SVs by aligning reads from sequencing on a pan-genome representing the combination of several
493 genomes [14, 20, 22, 52]. However, genotyping InDels with high reliability and call rate by these
494 approaches required at least 30X-50X coverage of the genome to correctly cover their breakpoint and
495 their internal sequence, especially to genotype InDels larger than 50bp [52]. Additionally, aligning reads
496 from a thousand individuals on a pan-genome remained computationally intensive, and therefore
497 required large informatics facilities [52]. In the end, these approaches required to build a pan-genome of
498 high-quality, which remains challenging for a complex genome.

499 In this paper we describe a new approach combining (i) the ‘accuracy’ of detecting InDels using whole
500 genome assembly, with the detection of 89,150 insertions and 52,175 deletions from the comparison of
501 three newly sequenced and assembled maize inbred line (F2, PH207, and C103) genomes and the public
502 maize B73 AGPv2 reference genome, (ii) and the ‘high-throughput’ genotyping utility provided by SNP
503 arrays. This approach allowed us to genotype, for the first time, thousands of insertion/deletion variants,
504 including PAVs, on a few hundred maize individuals. Genotyping cost per individual using the InDel array
505 was at least 10-20 fold cheaper than any approach based on sequencing for a species with a genome as

506 complex as maize, at a similar level of reliability (> 1000€-2000€ for a 30-50X of a 3Gbp genome vs 50€-
507 220€ using Affymetrix® Axiom® array, depending on the number of samples and probes). This genotyping
508 cost did not include bioinformatics analysis. Calling SVs from a pan-genome of a species with a large and
509 complex genome, such as maize, was time-consuming and required bioinformatics skills and large
510 informatics facilities, which are costly and not available in all laboratories. In the contrary, the array could
511 be analyzed rapidly on a laptop using a pipeline already implemented for analyzing SNPs and the
512 Hom2OTV R script developed for analyzing MONO probes. Additionally, the array provided a wet-lab
513 validation of the InDel discovery and allowed the removal of putative genotyping errors from sequencing
514 (particularly for PAVs), due to incomplete or bad genome assembly, as we observed in our study. In the
515 end, the probe content of the InDel array can be largely optimized, either to reduce the size of array (and
516 therefore the cost), or to increase the number of SVs genotyped, without losing reliability (e.g. 200,000
517 to 300,000 InDels) by filtering out under-performing probes, by strongly reducing the number of probes
518 per InDel (2-3), and by removing false positive InDels. It would also be easy to design an array combining
519 probes targeting InDels and more classical SNPs, outside of InDel sequences.

520 With the use of breakpoint probes for both insertions and deletions, our approach overcomes some
521 of the limitations of previous CGH or SNP array-based studies, which were only able to call deletions if a
522 few successive probes had lower fluorescent intensity signals [32–35]. Unterseer et al., (2014) genotyped
523 specifically 6,759 small deletions, which were discovered by aligning reads of 30 inbred lines against the
524 B73 genome, but the study did not include any insertions [37]. However, previous CGH and SNP arrays did
525 not design probes to target breakpoints and detected InDels by analyzing the variation of fluorescent
526 intensity signals of ordered probes [32–34]. Consequently, these technologies targeted exclusively low
527 copy regions of the genome, excluding InDels containing repeats, such as transposable elements (TEs) [2,
528 30, 44]. This is a strong drawback for maize and many other crops since a large part of their sequence is
529 composed of transposable elements [28, 59] which may be highly variable between individuals [4, 24, 60]
530 and may impact phenotypes [61–63]. The use of BP probes allows to target Present/Absent Variations,
531 whose sequence are unique and not present elsewhere in the genome, as well transposable elements,
532 whose internal sequence can be present/absent at one specific locus but also present elsewhere in the
533 genome. Another advantage of genotyping breakpoints is that it provides the ability to genotype the same
534 mutational event across all individuals of the population, as it is highly unlikely that two independent
535 mutational events could lead to the exact same breakpoint. On the contrary, for InDels detected using
536 classical CGH or SNP arrays, it is much harder to identify common InDels among a population of
537 individuals, as we don't know precisely their breakpoints. Genotyping breakpoints is also very cheap since
538 only one or two probes are needed, which makes the InDel size no longer a limitation for genotyping it
539 accurately, contrary to previous SNP and CGH arrays that rely on fluorescent intensity variation of probes
540 covering the entire InDel sequence [45]. The genotyping of breakpoints by sequencing is possible with a
541 tool like PInDel [50], which has a genotyping mode or BayesTyper [52], but at a much greater cost and
542 with lower call rate compared to the use of a SNP array. Finally, breakpoint probes are codominant
543 markers and allow accurate genotyping of hemizygous individuals (Heterozygous for presence/absence),
544 since their genotyping is based on fluorescent contrast rather than fluorescent intensity variation, which
545 is known to be noisier as with MONO and OTV probes [45].

546 Although the use of BP probes is clearly the simplest way to genotype InDels using an SNP array,
547 breakpoints are not always available (“no map” approach discovery) or “designable” with 35bp probes,
548 for instance, the cases where sequences of microhomology at breakpoint site were larger than 5bp. In
549 order to genotype the 52,471 InDels without breakpoints and explore the genetic diversity within InDels,
550 we also designed 577,778 internal probes both on monomorphic and polymorphic sites in PARs for both
551 insertions and deletions. To genotype PARs in InDel sequences using SNPs, we took advantage of the
552 already available Affymetrix® algorithms to call Off-Target Variants (OTVs), which can detect variation of
553 fluorescent intensity signals for a single probe (Figure 1C) [36]. This approach was used by [37] who was
554 able to detect 45,974 OTVs on a set of diverse maize inbred lines using a 600K SNP array. Nevertheless,
555 the array was designed in a classical way to target SNPs, and there was no prior evidence that the probes
556 called as OTVs would belong to InDels. Additionally, detecting SNPs in insertions required the assembly of
557 a pan-genome, combining common and specific sequences from different individuals, in order to retrieve
558 SNPs by aligning reads from sequenced lines [14, 20, 22, 52]. In our case, only using OTV probes would
559 have resulted in the elimination of many InDels, since 87,372 of them, including 74,648 insertions, did not
560 have known SNPs within their sequence. In order to avoid this ascertainment bias due to prior knowledge
561 of the presence of SNPs we designed 414,500 MONO probes on putative monomorphic sites within PARs
562 of InDel sequences. This permitted the genotyping of 38,134 supplementary InDels that could not be
563 targeted by OTV or BP probes. This new type of probe required the development of a new algorithm in
564 order to cluster individuals according to their fluorescent intensity variation only, to be able to assign a
565 genotype to each individual (Additional file 2: Figure S7C). A limitation of current workflow is that
566 Affymetrix® algorithms require a larger number of hemizygous individuals to generate high-quality
567 genotype clusters using the OTV and MONO probes. While it was not an issue for maize inbred lines (or
568 individuals from autogamous species) that are mostly homozygous, it was an issue for individuals from
569 allogamous species that are highly heterozygous. By using alternate genotyping techniques or processing
570 a larger number of hemizygous samples, it should be possible to identify hemizygous clusters according
571 to fluorescence intensity from OTV and MONO probes. We observed some clusters that seem incorrectly
572 interpreted as heterozygote for SNPs, although they likely correspond to hemizygous individuals for OTV
573 and MONO probes (Additional file 2: Figure S9B, see below for a more detailed discussion). Alternatively,
574 other algorithms/software based on fluorescent intensity variation of either a single probe or several
575 ordered probes exist and could be used to detect copy number variation for hemizygote individuals [38–
576 43].

577 In the end, we observed some ascertainment bias using our array (Figure 5). This was due to the fact
578 that our four inbred lines do not well represent the whole genomic diversity of maize, notably missing are
579 tropical lines. As a consequence, it could lead to ascertainment bias by reinforcing the differentiation of
580 inbred lines genetically close to the four inbred lines used to discover InDels [54, 64, 65] as we observed
581 in our diversity analysis for lines close to B73 and F2 (Figure 5 and Figure S13). It could be therefore highly
582 valuable to use more lines for the initial InDel discovery step. Several new individual maize genome
583 assemblies are now available in the public domain and more and more could become available in the
584 future. Our approach could easily be applied to these new genome assemblies to discover new InDels on
585 a larger set of inbred lines representative of maize diversity with the aim to design a new InDel array.

586 2. Reliability of genotyping / calling results

587
588 Our approach provides a reliable and reproducible method for genotyping InDels in inbred lines, since
589 (i) the genotypes obtained by array and by sequencing were highly consistent for BP probes (97%) and in
590 a lesser extent with OTV and MONO probes (92% and 88%, respectively), due to the fact that the genome
591 assembly of sequenced lines were incomplete or incorrect, resulting in high error rates for absent calls
592 using GBS ; (ii) the average probe genotyping error rate was estimated at 3% (lower for absent calls); (iii)
593 the InDel genotyping errors could be greatly reduced by combining the genotypes of different probes
594 within the InDels (0.02% for 5 probes); (iv) the genotyping results were highly reproducible between DNA
595 replicates of F1 hybrids (95 to 97%, depending on probe type) and between inbred lines (94.8 to 99.4%);
596 and (v) the call rate for individuals was very high (96 to 99%) and can be increased by combining the
597 genotypes of the probes within the InDels (97.7 to 99.9% for 2 and 5 probes, respectively).

598 Our approach is promising as a method to genotype structural variations in maize, as well as other
599 species with complex genomes. We obtained high metrics, comparable to classical SNP arrays, based on
600 Affymetrix® Axiom® Technologies, even though InDels are more complex to genotype. First, call rates are
601 high and quite similar to those obtained for SNP with the 600K SNP Affymetrix® array (98% against 98.1%
602 in [37]). Nevertheless, we observed a lowest call rate for BP probes (90%). This lowest call rate could be
603 explained by the usage of more relaxing criterion to filter out probes for building array and by the fact
604 that polymorphisms in surrounding sequences of InDel breakpoints have not been taken into account
605 contrary to internal probes. Second, the percentage of BP and OTV probes classified as PHR (94% in both
606 cases) is similar than for 600K SNP Affymetrix® genotyping array (92%) but higher than for 1.2M screening
607 Affymetrix® arrays (~65%) that have been used to select best markers for designing the final 600K SNP
608 Affymetrix® arrays. It is difficult to compare the classification of MONO probes, because the algorithm
609 used (Hom2OTV) is new and quite different from the one used for BP, OTV, and classical SNPs. Third, the
610 reproducibility between DNA replicates of F1 hybrids was high (95 to 97%, depending on probe type), but
611 this is lower than for SNP arrays (~99.5% in [37]). However, the reproducibility was estimated on DNA
612 replicate of F1 hybrids in our study while it was estimated on inbred lines for 600K SNP Affymetrix® array.
613 When we compared genotype of 13 inbred lines originated from different seedlots, reproducibility is close
614 to those of 600K SNP Affymetrix® array (98.3%) and displayed approximatively same reproducibility with
615 50K SNP Illumina array ([54], Additional file 1: Table S9). This comparison suggested strongly that our
616 lower reproducibility might not be due to genotyping errors but possibly the divergence between the
617 samples for inbred lines and the use of F1 hybrids rather than inbred lines for DNA replicate. Fourth, the
618 Mendelian inheritance between F1 hybrids and their parental lines was lower for our InDel than for SNP
619 array (88% vs 97.6% in [37]) but quite similar considering only homozygous genotypes (95%). This is likely
620 due to the presence of a small number of hemizygous samples since the 16 F1 hybrids were eliminated
621 due to their low call rate (<0.9) and there are only residual hemizygosity for inbred lines. Considering the
622 F1 hybrids for defining BP cluster could improve the delineation of hemizygous cluster and therefore
623 Mendelian inheritance. Note that 600K SNP Affymetrix® in maize was designing by selecting the high
624 confidence probes based on results of a first screening 1.2M SNP Affymetrix® array which could favor
625 reproducibility for this array. Finally, 72% of probes were converted into markers, which is comparable to
626 this 1.2 maize Affymetrix® Axiom® SNP screening arrays (74.9% in [37]). Out of these, 88% were

627 polymorphic for presence/absence. This conversion rate is expected, considering that Affymetrix® Axiom®
628 array analysis pipelines have been optimized for the detection of bi-allelic SNPs and are more sensitive to
629 variations in fluorescent contrast (x-axis) compared to variations in fluorescent intensity (y-axis), which is
630 known to be noisier [36, 45]. Moreover, we did not always follow Affymetrix® recommendations, as we
631 did not filter out probes with a bad design score.

632 We identified some inconsistencies between genotyping by array (GBA) and genotyping by
633 sequencing (GBS) obtained by aligning probes against our genomes (Table 4). These inconsistencies were
634 higher when GBS called absent for InDels interrogated by OTV and MONO probes (17.1% and 20.2% vs.
635 4.3% and 5.4%, respectively), although no differences were observed for BP probes (Table 4). These biased
636 inconsistencies towards absence for internal probes seems very high compared to our analysis on the
637 consistencies between probes within Indels. Our analysis of consistencies between probes within InDels
638 showed indeed that genotyping errors produced by the array were close to 3% (Figure 4) and lower for
639 absent calls (Additional file 2: Figure S12). These results suggested that the higher genotyping
640 inconsistencies for GBS absent are due to errors in GBS. GBS errors for absence were well explained by
641 the use of an incomplete genome draft assembly to align probes sequences, and the use of a higher-
642 quality genome could help to reduce these inconsistencies. The probes targeting sequence regions
643 present in one line, but not assembled in their draft genome assemblies, were falsely genotyped absent,
644 but the sample DNA correctly hybridized with the probes, and the InDels were called present with the
645 array. This could also explain why the number of inconsistencies was higher for B73, as all B73 absence
646 genotypes were defined in comparison to draft assemblies. Whereas for the other 3 lines, absence
647 genotypes were defined in comparison with the gold standard B73 genome sequence. The fact that we
648 obtained a better result on OTV probes interrogating InDels discovered in F2 can be explained because
649 we used only SNPs discovered on the B73-F2 pan-genome and not in other genomes. And, the fact that
650 BP probes had similar consistencies for genotyping absent and present calls could be explained by the fact
651 that the BP probes were designed exclusively on B73 reference genome.

652 We also found that 20,574 InDels were monomorphic and present across all lines, suggesting they
653 represented false positives from regions not assembled in our draft genomes. To reduce this false positive
654 rate, we strongly advise to not only align B73 reads onto each draft genome assembly but to also align
655 reads from each sequenced genome on each other and against itself. This would have several benefits: (i)
656 it would allow to discover even more and higher-quality InDels, as each putative deletion discovered in
657 one sample could potentially benefit from supporting reads from another sample; (ii) this would simplify
658 the identification of InDels common to more than one genotype; and (iii) it would help to identify and
659 eliminate false positive deletions by the alignment of each sample on its own draft assembly.

660 Nevertheless, the use of incomplete draft genomes does not explain all discrepancies between
661 genotypes obtained by sequencing and by array. First, these discrepancies could also be due to incorrect
662 clustering and assignment of a genotype call (array errors). This was exemplified by some MONO probes
663 classified as SNPs, although the clustering pattern looks like a MONO cluster with a large difference of
664 fluorescence intensity between two clusters (Additional file 2: Figure S9C). A more detailed inspection of
665 the clustering of MONO probes displayed an unexpected cluster pattern (Table 4, Additional file 2: Figure
666 S9D), and OTV probes classified as SNPs (Table 4, Additional file 2: Figure S9A) suggests a wrong

667 assignment of genotypes for the cluster displaying the lowest fluorescent intensity. Similarly, the genome
668 divergence within probe sequences for some inbred lines could result to group those individuals in an OTV
669 cluster, and therefore result in an incorrect absent call. However, these genotyping errors due to bad
670 clustering or genomic divergence between individuals within probes sequences could be strongly reduced
671 by combining genotypes from several probes. As an InDel called by five different probes has a random
672 genotyping error of 5%, we showed by simulation that the genotyping error for that InDel would be
673 reduced to 0.1%, when the most frequent allele among the 5 probes was assigned as genotype of the
674 InDel (Additional file 1: Table S6).

675 Surprisingly, 4.7% of MONO probes displayed a classical OTV clustering, suggesting that an unknown
676 SNP was targeted by these probes by chance. This high level of polymorphism (1 SNP / 21 bp) was slightly
677 higher than observed by sequencing a small set of diverse lines [66, 67]. It could suggest that PAR genomic
678 regions might have more divergence than other parts of the genome, because these regions were involved
679 in local adaptation by maintaining together favorable combinations of alleles as proposed by [68]. These
680 15,690 new OTVs are very interesting, since they were discovered by chance on a large set of 445 inbred
681 lines. We could therefore expect that these OTVs have no ascertainment bias, which can be very useful
682 for analyzing genetic diversity within InDels carrying PAR regions. In addition, 20.4% of MONO probes
683 displayed unexpected clustering: one off-target cluster, corresponding to absence of the sequence; one
684 homozygous cluster, corresponding to presence of the sequence; and an unexpected heterozygous cluster
685 (Unexpected MONO 1 in table 4). Considering these “unexpected MONO 1” as true SNPs would indicate
686 a density of 1 SNP every 5 bp, which is not compatible with the level of diversity observed in previous
687 studies of maize [66, 67]. Deeper investigation of these MONO probe clusters identified that for some
688 probes, the unexpected heterozygous cluster is positioned between the presence and absence clusters
689 (Additional file 2: Figure S9B). This suggests that these unexpected heterozygous clusters are identifying
690 inbred samples with only one copy presence (hemizygous genotype). An alternative hypothesis to explain
691 this unexpected pattern is the presence of divergent duplicated sequences, leading to the existence of an
692 artificial heterozygous cluster for SNPs corresponding to the presence of two paralogous sequences. This
693 result suggests therefore that there is probably room to develop genotyping strategies in order to better
694 identify additional clusters corresponding to the presence of hemizygous individuals for both MONO and
695 OTV probes and therefore improve the quality of the genotyping of InDels when using a SNP array.

696 These potential clustering errors, as well as the incorrect design of some probes, can explain some
697 inconsistent genotypes for presence/absence between probes for the same InDel. Comparison of
698 genotyping across different probes within InDels could help to identify and remove probes displaying
699 highly discordant genotypes, due to errors originating from poor clustering or from poor design.
700 Interestingly, some InDels showed reproducible inconsistent genotypes for presence/absence across their
701 probes in several inbred lines (Additional file 2: Figure S9B). This suggested that this pattern could have a
702 biological origin, with possible rearrangements having occurred several times within the same genomic
703 region in some inbred lines. Following this hypothesis, Gu et al. (2008) observed two different types of
704 rearrangements which could explain our observations [69]: (i) rearrangements with an unique breakpoint
705 in population and therefore common size between individuals resulting to two haplotypes in a population
706 and (ii) rearrangement with non-unique breakpoints, scattered in a genomic region, which resulted in

707 several haplotypes. This hypothesis is also supported in our experiment by the 56% of BP probes classified
708 as OTVs, indicating that FW or/and REV flanking sequence did not hybridize in some lines.

709 The development of a statistical approach to merge either *a posteriori* the calling results of
710 independent clustering of individual probes or *a priori* the fluorescent intensity signal of successive probes
711 within a InDel could be interesting in order to improve the robustness of InDel genotyping. This would
712 have the advantage to limit the effect of genotyping errors due to poor clustering and to reduce the noise
713 in fluorescent intensity signals. We showed by simulation that assigning the most frequent allele across
714 probes as the genotype reduced genotyping error to 0.7% and 0.1% when 3 and 5 probes were used,
715 respectively. Additionally, it increases the InDel call rate (Additional file 1: Table S6). In the end, it would
716 also help to identify varying haplotypes, representing the complexity of a region in a population. Using
717 multiple probes for calling InDels is therefore highly valuable for improving reliability of InDel genotyping,
718 since it allows putatively to reduce random genotyping error, due to genomic divergence or other causes,
719 removes probes poorly clustered or designed, and identifies more complex rearrangements.

720 3. Conclusions

721
722 Our approach, from the sequencing of a few representative genotypes, their genome assembly, the
723 insertion/deletion discovery, and to the design and use of the high-throughput genotyping array was
724 applied to maize as a proof of concept. Our approach allowed us to rapidly create at a reasonable cost a
725 high-throughput SVs genotyping tool for this species. This approach will remain interesting as long as
726 calling large InDels from sequencing, for a large set of individuals, remains un-affordable, bioinformatically
727 challenging, and time-demanding. Nevertheless, our approach could benefit from few improvements
728 based on the knowledge accumulated from this test on maize. First, it could be highly valuable to use
729 more lines for the initial InDel discovery step to avoid ascertainment bias [64] as we observed in our
730 diversity analysis (Figure 5). Using more lines for detecting InDels should also reduce the number of false
731 positives SVs in array due to poor assembly, genotyping error due to genomic divergence between
732 individuals, and help to identify complex rearrangement. Second, even though we did not have any
733 indication that our sequenced data had been contaminated, a contamination cleaning step should be
734 applied to the sequenced data prior to SVs discovery and genome assembly, in order to avoid potential
735 false positive SVs in the final array. Third, aligning reads against the internal sequence of InDels, as well as
736 aligning probes sequences against each genome assemblies, should strongly reduce false positives in the
737 final array. Fourth, improving the pipeline of MONO and OTV probes to call hemizygous genotype from
738 variation of fluorescent data would be very valuable, notably for allogamous species. Fifth, capacity of
739 array could be largely increased to 200,000 or 300,000 InDels without losing reliability by optimizing
740 number of probes per InDels.

741 To conclude, we developed a “proof of concept” high-throughput and affordable InDel genotyping
742 array, based on the InDels discovered by sequencing on four inbred lines. Our “proof of concept” approach
743 could be easily applied to other species to explore genomic structural variation, notably species with
744 limited sequence data or few genome assemblies available. This could also be interesting for species with
745 greater sequencing resources and where genotyping a large set of individuals is required, such as for

746 breeding purposes, genome wide association studies, genomic selection, or characterizing SVs in large
747 germplasm. Although our array was not designed to genotype duplications and inversions, our approach
748 could be easily extended to genotype breakpoints of inversions, but further development of the pipeline
749 for genotyping duplications using internal probes would be required. This powerful approach opens the
750 way to studying the contribution of InDels and other SVs to trait variation and heterosis in maize [44] and
751 should contribute to decipher the biological impact of InDels and other SVs at a larger scale in different
752 species.

753

754

755 Methods

756 Sequencing material

757 Three maize inbred lines, which are key founders of maize breeding programs and originated from
758 three different heterotic groups, had been selected for deep sequencing and InDel discovery: the
759 European Flint line F2 and two American dent lines, PH207 (Iodent) and C103 (Lancaster). For the F2
760 inbred line, see [20]. For C103 and PH207 inbred lines, DNA was extracted with the NucleoSpin Plant XL,
761 according to the manufacturer's instructions (Macherey Nagel, Düren, Germany). The DNA concentration
762 was estimated by UV measurement and the quality was checked with an agarose gel electrophoresis. Two
763 library types were sequenced: a 180bp overlapping paired-end library and a 3kb mate-pair library. The
764 paired-end libraries and the sequencing were performed by Integragen (Evry, France) on a HiSeq2000
765 sequencer (Illumina, San Diego, USA). 412 and 377 million 100bp paired-end reads (33x and 30x) were
766 sequenced respectively for C103 and PH207. The mate-pair libraries were prepared and sequenced at BGI
767 (China) also on HiSeq2000 sequencer (Illumina, San Diego, USA). Raw reads were filtered to remove
768 adaptor sequences, contamination, and low-quality reads. 326 and 316 million 100bp mate-pair reads
769 (26x and 25x) were sequenced, respectively for C103 and PH207. A data set of 473 million B73 inbred line
770 100bp paired-end reads (35x) with an average insert size of 191bp was downloaded from
771 <ftp://ftp.sra.ebi.ac.uk/vol1/fastq/SRR404/SRR404240>.

772 InDel and PAV discovery

773 For the deletion discovery step, F2, PH207, and C103 paired-end reads were aligned against B73
774 AGPv2 genome sequence using novoalign version 3.01.01 (<http://www.novocraft.com>) (default
775 parameters). Samtools [70] version 0.1.18 was used to coordinate, sort, and retain reads with a mapping
776 quality of at least Q30. Duplicated reads were eliminated using MarkDuplicate from the picardtools suite
777 (<http://broadinstitute.github.io/picard>) version 1.48. PInDel [50] version 0.2.5a2 was run in parallel on
778 each chromosome to perform multi-genotype calling of deletions. Raw formatted results were converted
779 to VCF (Variant Calling Format) using the script PInDel2vcf. BreakDancer [46] was used in complement
780 to PInDel, but only for F2. Deletions shorter than 100bp were discarded. Deletions spanning a B73 assembly
781 gap or located in regions prone to mis-assemblies, such as telomeric, knob, and centromeric regions, were
782 also excluded from further analysis using IntersectBed BEDTools [71] version 2.16.1.

783 For whole genome sequence reconstruction of F2, PH207, and C103 inbred lines, paired-end and
784 mate-pair reads were used together and assembled using ALLPATHs-LG [72] version R41008 (Additional
785 File 2: Figure S1B). For F2, the script CacheToAllPathsInputs.pl was used to cache the data to use for
786 assembly: 100% of the non-overlapping 230bp insert paired end data set, 100% of the overlapping 170bp
787 insert paired end data set, 30% of the non-overlapping 370bp insert paired end data set, and 100% of the
788 2.4kb insert mate pair data set. Indeed, only overlapping paired end reads are used by ALLPATHs-LG for
789 building contigs, but the supplementary non-overlapping paired end reads for F2 were used for error
790 correction. RunAllPathsLG was then run for all three genotypes using optional parameters. Details on the
791 sequence library usage during the assembly process are given in Additional file 1: Table S1. For each
792 assembly, the coverage of the gene space was evaluated using BUSCO [73] version 3.0.2 using genome
793 mode and the maize species (-m geno -sp maize).

794 B73 paired-end reads were successively aligned to ALLPATHs-LG F2, PH207, and C103 genome
795 sequence assemblies (Additional File 2: Figure S1B). The same tools and parameters used to call deletions
796 against the B73 genome were applied to detect B73 deletions against F2, PH207, and C103. Only insertions
797 smaller than 100bp were discarded, except those spanning real assembly gaps (with approximate size
798 inferred from paired reads average distance) and not “unsized” gaps like in the B73 genome. When
799 possible, insertions were anchored onto the B73 AGPv2 genome sequence using a dedicated pipeline
800 combining Megablast version 2.2.19 [74] and Age version 0.4 [75]. Again, insertions that could be
801 anchored on the B73 reference and were overlapping regions prone to mis-assemblies such as telomeric,
802 knob, and centromeric regions, were also excluded from further analysis using IntersectBed.

804 F2 specific sequences coming either from the no map approach (Additional file 2: Figure S1) or
805 from the work of [20] were included as such, without any further filtering.

806 The multiple references and approaches used during the InDel discovery step led to a set of InDels
807 with various levels of redundancy. Some “intra-tool” redundancy was found (e.g. multiple calls found by
808 one tool within the same genotype at highly polymorphic loci). These “ambiguous” calls were
809 systematically identified using the Bedtools suite version 2.16.1 [71] and eliminated. Moreover, for F2
810 deletions, some “inter-approach” redundancy was also expected and eliminated using intersectBed utility
811 also from the Bedtools suite. When redundancy was found, PInDel calls were preferred to BreakDancer
812 calls, because they had precise breakpoints and contained the calls for PH207 and C103. The same filter
813 was applied to all insertions that could be anchored to the B73 genome sequence. Furthermore, for non-
814 anchored InDels, in order to avoid redundancy in internal genotyping probe design, RepeatMasker
815 (<http://www.repeatmasker.org>) was used to mask redundant regions by similarity using an iterative
816 approach. First, “ALLPATHs-LG assembly” F2 insertions were masked with “ABySS assembly” F2 insertions
817 (at least 95% of identity) to generate a non-redundant set of F2 insertions. Then C103 insertions were
818 masked with F2 insertions (at 90% of identity), PH207 insertions were masked with C103 and F2 insertions
819 (90%), and finally F2 no map specific sequences were masked with PH207, C103, and F2 insertions (90%).

820 Design of Affymetrix® Axiom® array

821 Preparation of sequences for probes for design

822 To identify presence/absence regions (PARs) within InDel sequences suitable for the design of
823 “off-target” probes, we used the genometools Tallymer utility [76] version 1.5.6 to create two indexes for
824 B73, F2, PH207, and C103: one from their genome assemblies (17-mers with a minimal occurrence of 1)
825 and one from a 5x genome equivalent subset of their raw sequenced data (17-mers with a minimal
826 occurrence of 5). Then B73 genome was iteratively annotated with the script tallymer2gff3.plx (options
827 used: -k 17 -min 35 -occ 1|5 depending on the index) to identify regions not covered by F2, PH207, and
828 C103 kmers. Reciprocally, the two F2 draft genomes, PH207 and C103 ALLPATHs-LG draft genomes were
829 run through the same procedure to identify regions not covered by B73 kmers. The gff files generated by
830 this process were then used in combination with gff files of repeats annotated with RepeatMasker to
831 define PARs of a minimum size of 35bp for each type of InDel and each draft genome.

832 BP preparation

833 Breakpoints could be targeted by probes (Figure 1A) provided that the nucleotide flanking the
834 breakpoint at the beginning of the deleted sequence was different from the nucleotide right after the end
835 of deleted sequence (and reciprocally on the reverse strand). Type I and type III breakpoints without
836 micro-homology sequence can be submitted for the Affymetrix® standard design procedure, whereas
837 type II breakpoints have to go through an iterative design process, shifting the sequence by one base on
838 each attempt until reaching a discriminative position. This iterative process stops after 5bp and is also
839 performed by Affymetrix®.

840 Probes scoring

841 All potential probes were evaluated in an *in-silico* analysis to predict their microarray
842 performance. A p-convert value, which arises from a random forest model intended to predict the
843 probability that the SNP will convert on the array, was determined for all probes. The model considers
844 factors including probe sequence, binding energies, and the expected degree of non-specific binding and
845 hybridization to multiple genomic regions. This degree of non-specific binding is estimated calculating 16-
846 mer hit counts, which is the number of times all 16 bp sequences in the 30 bp flanking region from either
847 side of the SNP have a matched sequence in the genome. These scores were generated both for forward
848 and reverse probes. A probeset is recommended if p-convert>=0.6 and there are no expected
849 polymorphisms in the flanking region. A probeset is neutral if p-convert>=0.4, the number of expected
850 polymorphisms in the flanking region is less than 3, and the polymorphisms are further than 21 bp of the
851 variant of interest. Probesets not falling into these two categories are scored as *not recommended*.
852 Probesets that cannot be designed are scored as *not possible*.

853 Probes selection

854 Concerning OTV and MONO probes, we applied three successive filtering steps. First, we selected
855 only probes classified as recommended and neutral based on their scoring, with no more than one hit on
856 the B73 reference genome for deletion probes, and no hit at all for insertion probes. After this step,
857 204,213 OTV probes and 18,884,827 MONO probes remained. Secondly, only probes with more than 70%

858 in PARs were kept. An additional filtering step was implemented specifically for MONO probes to optimize
859 probe distribution along the targeted PARs. For this step, PARs were split in 75bp windows using
860 windowmaker (Bedtools) and the MONO probe with the highest p-convert value was selected for each
861 window. If there were InDels with less than 4 MONO probes selected using 75bp windows, these probes
862 were eliminated and a second iteration was attempted, using 50bp windows, followed by a last iteration
863 with 25bp windows. This generated 616,286 probes including BP and OTV probes targeting 108,24 InDels
864 (90% of InDel selected for design). We completed the design by rescuing 6,219 OTV and 53,441 MONO
865 probes from InDels or PARs not targeted by any probes, bringing the total number of probes selected to
866 675,946 to target 109,292 InDel.

867 At the last step, duplicated probeset were removed based on their sequence by Affymetrix® during the
868 chip design procedure, leaving 662,772 probeset (105,927 InDels) corresponding to 1,404,570 different
869 probes to be tiled on the array.

870 Genotyping of 105k InDels on 480 maize DNA samples

871 Plant material for genotyping

872 For genotyping, 480 different DNA samples were extracted from leaves following a NaBisulfite
873 method modified from [77, 78]. These 480 samples included 440 inbred lines, 24 highly recombinant
874 inbred lines, and 16 F1 hybrids. Both F1 hybrids (obtained by crossing inbred lines) and their parental
875 inbred lines were genotyped on the array, but seed lots used to produce F1 hybrids and those used to
876 extract DNA for genotyping were different. Among these 480 DNAs, 13 inbred lines were genotyped using
877 two different DNAs from two different seed-lots and were used to evaluate the reproducibility of the
878 genotyping (Additional file 1: Table S9). DNA samples of one F1 hybrid were also genotyped 6 times.
879 Mendelian inheritance was estimated between 12 hybrids F1 derived from 9 different parental lines
880 (Additional file 1: Table S8)

881 Variant calling using Affymetrix® algorithm

882 Each type of probe had a dedicated algorithm (Additional file 2: Figure S7) to call genotypes,
883 according to expected behavior from the probe design. DNA samples from 480 individuals were hybridized
884 to the array using the Affymetrix® system. The genotyping, sample QC, and marker filtering were
885 performed according to the Axiom® Best Practice genotyping analysis workflow. Genotype calls and
886 classifications were generated from the hybridization signals in the form of CEL files using the Affymetrix®
887 Power Tools (APT) and the SNPolisher package for R, according to the Axiom® Genotyping Solution Data
888 Analysis Guide, and a custom-made R script, Hom2OTV, implemented the algorithm for calling MONO
889 probes.

890 The APT results were then post-processed using SNPolisher, which is an R package specifically
891 designed by Affymetrix®. Marker metrics were generated using the *Ps_Metrics* function. These marker QC
892 metrics were used to classify probesets into 14 categories (Additional file 2: Figure S8) using the
893 *Ps_Classification* and *Ps_Classification_Supplemental* functions, with all default setting for diploid (e.g.
894 *HetSO.cut*=-0.3, *HetvMAF.cut*=1.9), except for an empirically determined, more stringent heterozygous
895 variance filter (*AB.varY.Z.cut*=2.6). Example of clusters from each classification were visualized using the

896 *Ps_Visualization* function (Additional file 2: Figure S8). Variants were preferentially selected as
897 recommended if they were exhibiting stable category assignments with clearly separated clusters. Each
898 variant was ranked into a category (Additional file 2: Figure S8) at each step of the pipeline.

899 Algorithms used to convert BP and OTV were similar, as BP and OTV probes behaved like classical
900 SNPs. For initial genotype calling, *a priori* (generic) cluster positions were used, since no information about
901 expected positions was available. A first analysis was performed according to Affymetrix®
902 recommendations. Secondly, the level of inbreeding was taking into account for a posteriori cluster
903 definition, because of the high amount of inbred lines in the panel. This parameter took values from 0 for
904 fully heterozygous to 16 for completely homozygous samples. For OTV and BP algorithms, an inbred
905 penalty of 4 (lower penalty for inbred species) was applied to try to re-labelled probes that fall into
906 categories: CallRateBelowThreshold (CRBT), HomHomResolution (HHR), NoMinorHom (NMH), Other and
907 UnexpectedHeterozygosity, after the first cluster analysis (Additional file 2: Figure S8). Markers that were
908 classified as OTV may also be considered recommended after the *OTV_caller* function has been used to
909 re-label the genotype calls. The SNPolisher *OTV_Caller* function performed post-processing analysis to
910 identify miscalled AB clustering and identify which samples should be in the OTV cluster and which
911 samples should remain in the AA, AB, or BB clusters. Samples in the OTV cluster were re-labelled as OTV.
912 Finally, the recommended markers list is created by combining the list of markers that are classified into
913 the recommended categories (PolyHighResolution (PHR), MonoHighResolution (MHR), and OTV).

914 BP and OTV probes that exhibited only two clusters (AA or BB and OTV) should fall into the
915 monomorphic classification and be considered as not recommended. A new MONO algorithm was
916 developed (Figure 4), because, unlike traditional SNP genotyping, we only expected two clusters for
917 MONO probes (presence and absence) (Figure 1C). To classify monomorphic sequence genotyping, the
918 *OTV_Caller* function was called, and only MHR and NMH were considered as recommended. Other
919 monomorphic probes are then analyzed with an inbred penalty of 16 (highest level) to re-labelled probes
920 displaying higher-than-expected levels of heterozygosity. Finally, the new function called *Hom2OTV* was
921 implemented to classified probes exhibiting two homozygous clusters, with primarily an intensity
922 difference. This function determined if the intensity difference represents one homozygous cluster (InDel
923 presence) and one OTV cluster (InDel absence), as we expected. There are no parameters in this function.
924 The lower intensity homozygous cluster is recalled as OTV.

925 **Evaluation of genotyping quality**

926 We compared the genotyping for 479,027 probes from the InDel array (Genotyping By Array: GBA) with
927 the genotyping from sequencing (Genotyping By Sequencing: GBS) of 4 inbred lines used to discover the
928 InDels: B73, F2, PH207, and C103. Genotyping by sequencing was built from the alignment of probe
929 sequences on the reference genome B73 and the de novo assembly of 3 inbred lines (F2, PH207, and
930 C103) with Blast software. Sequences were considered present in lines when the probes were aligned
931 with less than 5% of mismatch or otherwise considered absent.

932 Genotyping consistency for B73, F2, PH207, and C103 was calculated between GBS and GBA according to
933 genotype calls “present” or “absent”, produced by GBS (Table 4). For this purpose, Affymetrix® genotyping
934 was converted into these genotypes: present, absent, and hemizygote (1 copy present). Consistency of

935 Presence/Absence genotypes between sequencing and array genotyping was analyzed for four individuals
936 (B73, F2, PH207, C103) according to probe types (BP, OTV, MONO): Number of similar genotypes between
937 GBS and GBA /number of genotype called by GBA and GBS. Note that the seed-lot used for B73 and F2
938 genotyping is different from the seed-lot used for InDel discovery, but it is the same seed-lot for inbred
939 lines PH207 and C103.

940 In order to evaluate the consistency of probe genotyping within InDels (Figure 4), we used 362 inbred
941 lines from an association panel representing a wide range of genetic diversity (Camus-Kulandaivelu, 2005;
942 Bouchet et al., 2013). From 479,027 probes, we selected 294,650 polymorphic probes and fully consistent
943 between GBS and GBA in order to limit the genotyping errors due to sequencing. These probes genotyped
944 72,555 InDels. We then selected 50,648 polymorphic InDels that are genotyped with at least two probes
945 (corresponding to 270,581 probes), and calculated the average frequency of the presence allele across all
946 probes for each InDel and inbred line. For each InDel, we calculated the frequency of inbred lines
947 displaying fully consistent genotypes between probes, *i.e* the proportion of lines where the average
948 frequency across all probes is 0 or 1. We also calculated frequency of inbred lines that have a least one
949 probe with an inconsistent genotype (FreqDiff01), *i.e* the proportion of lines where the average frequency
950 across all probes is not 0 or 1. To evaluate the effect of the probe numbers on the frequency of lines
951 inconsistent within InDels, we analyzed the variation of frequency of lines not fully consistent (FreqDiff01)
952 with relation to the number of probes within the InDels, by estimating median and average FreqDiff01 for
953 each probe count (Figure 4B, Additional file 1: Table S5). To estimate the probe genotyping error rate, we
954 compared this variation to what we could expect for different genotyping error rates (1, 3, 5, and 10%) in
955 362 lines, genotyped by 10,000 Indels, with the number of probes varying from 2 to 50, using a binomial
956 sampling (Additional file 1: Table S6). For this, we simulated a number of false genotypes among the
957 probes for each InDel and each line using the rbinom function in R, with the following parameters:
958 Number of observation = 362 lines x 10,000 Indels; Number of trials for each observation = Number of
959 probes; Probability of success of each trial = probes genotyping error rate. Using this simulation, we
960 estimated frequency of inconsistent calls among 362,000 simulated genotypes (FreqDiff01) for each
961 probes count, varying from 2 to 50, and compared them with the median and average FreqDiff01 (Figure
962 4). To evaluate the impact of combining multiple probes for a genotype to correct genotype errors, we
963 used this simulation to estimate the InDel genotyping error rate, if we assign, to an inbred line, the most
964 frequent allele, based on the average allelic frequency of presence (Additional file 1: Table S6). To
965 compare accuracy for genotyping absence and presence using this array, we separated the InDels in four
966 classes, according to their average allelic frequency of absence in 362 inbred lines (0-25%, 25%-50%, 50%-
967 75%, 75%-100%) and compared their median FreqDiff01 (Additional file 2: Figure S12).

968 To evaluate the reproducibility of the 479,027 probes on the array, we compared the genotypes between
969 6 DNA replicates from F1 hybrids that originated from crossing B73 and F72. We also compared the
970 genotypes of 13 duplicated inbred lines (A554, A632, A654, B73, C103, CO255, D105, EP1, F2, F252, KUI3,
971 Oh43, and W117) that originated from different seed sources (Additional file 1: Table S9). The genotypes
972 of these 13 duplicated lines were also compared using 43,982 SNPs from the Illumina 50K SNP array.

973 To evaluate the quality of genotyping, we also analyzed 12 F1 hybrids derived from 9 parental inbred lines
974 (Additional file 1: Table S8). We first predicted the genotypes of the 12 F1 hybrids, based on the genotyping

975 of their 2 parental lines, for 46,382 BPs probes, removing OTV calls. These predicted genotypes were then
976 compared with the observed genotypes of the corresponding hybrids: Number of similar genotypes
977 (homozygous or hemizygous) between predicted and observed/Number total of genotypes. BP probes
978 producing missing data or displaying hemizygous genotypes in the parental lines were excluded from the
979 comparison. Note that the seed-lots of the parental inbred lines genotyped may have been different from
980 the seed-lots used for producing the F1 hybrids.

981

982 Diversity analysis

983 We performed diversity analysis on 362 inbred lines from an association panel representing a
984 wide range of diversity [55, 57], obtained using InDels genotyped on our InDels Affymetrix® Axiom® array
985 and using SNPs genotyped from the Illumina 50K SNP array [54]. The genotypes of InDels were treated as
986 bi-allelic “present” and “absent”.

987 To perform diversity analysis, we first selected 237,629 probes among the 479,027 probes for
988 which (i) the clustering observed were consistent with expectation (Table 3) and (ii) for which genotypes
989 produced by our array for the 4 lines used for discovering the InDels were fully consistent with the
990 genotyping, based on the alignment of the probes on the genome assemblies using BLAST software. We
991 filtered out 219,068 probes based on their genotyping quality (missing data rate below 20%, heterozygous
992 rate below 15% and minor allele frequency above 5%). In the end, we selected a single, best probe for
993 each InDel, leading to a set of 57,824 probes genotyping 57,824 InDels to analyze diversity in 362 inbred
994 lines.

995 We estimated two kinship matrices between 362 lines using “identity by descent” estimators (IBD)
996 based on 57,824 InDels and on 28,143 prefixed Panzea SNPs from the Illumina 50K (Figure 5). Kinship
997 matrices were estimated with the “ibd” function in the R package GenABEL [79]. We performed
998 correlation between IBD values estimated with SNP and InDel polymorphisms. Genetic structuration was
999 estimated using only the 28,143 Panzea SNPs with admixture software [80]. We selected the admixture
1000 results for five genetic groups (Q=5), since it corresponded to the number of genetics groups defined in
1001 previous studies using the Panzea SNPs from the Illumina 50K [55]. Lines were assigned to one genetic
1002 group, given that the probability of assignment to the groups was greater than 0.6, whereas lines below
1003 this threshold were considered “admixed”. In order to compare genetic structuration based on InDels and
1004 SNPs, we performed Principal Coordinate Analysis (PcoA) on genetic distance between lines with (362
1005 lines) and without F2 and B73 (360 lines) based on their dissimilarity (1-IBD) using InDels. Each line was
1006 plotted on the first two planes of PcoA and colored according to the assignment to the 5 genetics groups
1007 (Figure 5).

1008

1009 List of abbreviations

1010 GBA = Genotyping by array
1011 GBS = Genotyping by sequencing
1012 SNP = Single nucleotide polymorphism
1013 InDel = Insertion / Deletion
1014 BP = Breakpoint
1015 MONO = Monomorphic
1016 OTV = Off Target Variant
1017 QC = Quality control
1018 PHR = Poly High Resolyion
1019 VCF = Variant Call Format
1020 PAR = Presence / Absence Region
1021 PAV = Presence / Absence Variant
1022 SV = Structural variant
1023 CNV = Copy Number Variant
1024 TE = Transposable Element
1025 CGH = Comparative Genomic Hybridization
1026 NGS = Next Generation Sequencing
1027 FW = Forward
1028 REV = Reverse
1029 NAM = Nested Association Mapping
1030 DNA = Deoxyribonucleic Acid
1031 PCR = Polymerase Chain Reaction
1032 PcoA = Principal Coordinate Analysis
1033 Mbp = Millions of Base Pairs

1034 bp = base pair
1035 FreqDiff01 = Frequency of lines not fully consistent between probes within InDel
1036

1037 **Declarations**

1038 **Ethics approval and consent to participate**

1039 Not applicable

1040 **Consent to publish**

1041 Not applicable

1042 **Availability of data and materials**

1043 The array content is available at <https://doi.org/10.15454/DWB4UT>

1044 **Competing interests**

1045 Ali Pirani is an employee of Thermo Fisher Scientific (formerly Affymetrix®).

1046 **Funding**

1047 This work was supported by the project CNV-MAIZE (ANR-10-GENM-003) and the project Investement
1048 for the future AMAIZING ANR-10-BTBR-01 (ANR-PIA AMAIZING) and France Agrimer. PhD student C.
1049 Mabire is jointly funded by the program CNV4sel in the framework of metaprogram Selgen and by the
1050 Plant Biology and Breeding department of the French National Institute for Agricultural Research (INRA).

1051 **Authors' contributions**

1052 SDN designed and supervised the study and conducted CNVMaize project. CM, JD, and SDN drafted and
1053 corrected the manuscript, CV and JJ corrected the manuscript. NR, SDN, JPP, and SP conceived the array,
1054 AP, SDN, JJ and JD designed the array. AP developed the Affymetrix® genotype calling software and
1055 preformed the InDel genotype calling. JPP, JJ, and CV contributed to the sequencing; JD, AD, HR, and JJ
1056 performed the InDel discovery, JD and JJ build genome assemblies, JJ and AD discovered SNP within the
1057 InDels. CM evaluated the quality of genotyping and conducted the genetic diversity analysis. DM and VC
1058 did DNA extraction and prepared the samples for arrays genotyping. All authors have read and approved
1059 the manuscript.

1060 **Acknowledgements**

1061 We are very grateful to Patrick Schnable and Cheng-Ting “Eddy” Yeh for providing a subset of
1062 Presence/Absent Variants coming from their RNAseq and Sequence capture approach and for his helpful

1063 discussion. We are very grateful to Alain Charcosset for their contribution to the choice of inbred lines
1064 genotyped by the array and for his helpful discussion and comments on the manuscript.

1065 References

- 1066 1. Anderson JE, Kantar MB, Kono TY, Fu F, Stec AO, Song Q, et al. A Roadmap for Functional Structural
1067 Variants in the Soybean Genome. *G3amp58 GenesGenomesGenetics*. 2014;4:1307–18.
- 1068 2. Beló A, Beatty MaryK, Hondred D, Fengler KevinA, Li B, Rafalski A. Allelic genome structural variations
1069 in maize detected by array comparative genome hybridization. *Theor Appl Genet*. 2010;120:355–67.
- 1070 3. Cao J, Schneeberger K, Ossowski S, Günther T, Bender S, Fitz J, et al. Whole-genome sequencing of
1071 multiple *Arabidopsis thaliana* populations. *Nat Genet*. 2011;43:956–63.
- 1072 4. Liu J, Qu J, Yang C, Tang D, Li J, Lan H, et al. Development of genome-wide insertion and deletion
1073 markers for maize, based on next-generation sequencing data. *BMC Genomics*. 2015;16:601.
- 1074 5. Owens GL, Baute GJ, Hubner S, Rieseberg LH. Genomic sequence and copy number evolution during
1075 hybrid crop development in sunflowers. *Evol Appl*. 2019;12:54–65.
- 1076 6. Saintenac C, Jiang D, Akhunov ED. Targeted analysis of nucleotide and copy number variation by exon
1077 capture in allotetraploid wheat genome. *Genome Biol*. 2011;12:R88.
- 1078 7. Saxena RK, Edwards D, Varshney RK. Structural variations in plant genomes. *Brief Funct Genomics*.
1079 2014;13:296–307.
- 1080 8. Springer NM, Ying K, Fu Y, Ji T, Yeh C-T, Jia Y, et al. Maize Inbreds Exhibit High Levels of Copy Number
1081 Variation (CNV) and Presence/Absence Variation (PAV) in Genome Content. *PLoS Genet*.
1082 2009;5:e1000734.
- 1083 9. Swanson-Wagner RA, Eichten SR, Kumari S, Tiffin P, Stein JC, Ware D, et al. Pervasive gene content
1084 variation and copy number variation in maize and its undomesticated progenitor. *Genome Res*.
1085 2010;20:1689–99.
- 1086 10. Chia J-M, Song C, Bradbury PJ, Costich D, de Leon N, Doebley J, et al. Maize HapMap2 identifies
1087 extant variation from a genome in flux. *Nat Genet*. 2012;44:803–7.
- 1088 11. Mace ES, Tai S, Gilding EK, Li Y, Prentis PJ, Bian L, et al. Whole-genome sequencing reveals untapped
1089 genetic potential in Africa's indigenous cereal crop sorghum. *Nat Commun*. 2013;4:2320.
- 1090 12. Hirsch CN, Foerster JM, Johnson JM, Sekhon RS, Muttoni G, Vaillancourt B, et al. Insights into the
1091 Maize Pan-Genome and Pan-Transcriptome. *Plant Cell*. 2014;26:121–35.
- 1092 13. Lu F, Romay MC, Glaubitz JC, Bradbury PJ, Elshire RJ, Wang T, et al. High-resolution genetic mapping
1093 of maize pan-genome sequence anchors. *Nat Commun*. 2015;6.
1094 <http://dx.doi.org/10.1038/ncomms7914>.

1095 14. Montenegro JD, Golicz AA, Bayer PE, Hurgobin B, Lee H, Chan C-KK, et al. The pangenome of
1096 hexaploid bread wheat. *Plant J.* 2017;90:1007–13.

1097 15. Zhao Q, Feng Q, Lu H, Li Y, Wang A, Tian Q, et al. Pan-genome analysis highlights the extent of
1098 genomic variation in cultivated and wild rice. *Nat Genet.* 2018;50:278–84.

1099 16. Hardigan MA, Crisovan E, Hamilton JP, Kim J, Laimbeer P, Leisner CP, et al. Genome Reduction
1100 Uncovers a Large Dispensable Genome and Adaptive Role for Copy Number Variation in Asexually
1101 Propagated *Solanum tuberosum*. *Plant Cell.* 2016;28:388–405.

1102 17. Varshney RK, Saxena RK, Upadhyaya HD, Khan AW, Yu Y, Kim C, et al. Whole-genome resequencing
1103 of 292 pigeonpea accessions identifies genomic regions associated with domestication and agronomic
1104 traits. *Nat Genet.* 2017;49:1082–8.

1105 18. Belo A, Zheng P, Luck S, Shen B, Meyer DJ, Li B, et al. Whole genome scan detects an allelic variant of
1106 *fad2* associated with increased oleic acid levels in maize. *Mol Genet Genomics.* 2008;279:1–10.

1107 19. Hirsch CN, Hirsch CD, Brohammer AB, Bowman MJ, Soifer I, Barad O, et al. Draft Assembly of Elite
1108 Inbred Line PH207 Provides Insights into Genomic and Transcriptome Diversity in Maize. *Plant Cell.*
1109 2016;28:2700–14.

1110 20. Darracq A, Vitte C, Nicolas S, Duarte J, Pichon J-P, Mary-Huard T, et al. Sequence analysis of
1111 European maize inbred line F2 provides new insights into molecular and chromosomal characteristics of
1112 presence/absence variants. *BMC Genomics.* 2018;19:119.

1113 21. Jiao Y, Peluso P, Shi J, Liang T, Stitzer MC, Wang B, et al. Improved maize reference genome with
1114 single-molecule technologies. *Nature.* 2017. doi:10.1038/nature22971.

1115 22. Pinosio S, Giacomello S, Faivre-Rampant P, Taylor G, Jorge V, Le Paslier MC, et al. Characterization of
1116 the Poplar Pan-Genome by Genome-Wide Identification of Structural Variation. *Mol Biol Evol.*
1117 2016;33:2706–19.

1118 23. Appels R, Eversole K, Stein N, Feuillet C, Keller B, Rogers J, et al. Shifting the limits in wheat research
1119 and breeding using a fully annotated reference genome. *Science.* 2018;361:eaar7191.

1120 24. Sun S, Zhou Y, Chen J, Shi J, Zhao H, Zhao H, et al. Extensive intraspecific gene order and gene
1121 structural variations between Mo17 and other maize genomes. *Nat Genet.* 2018;50:1289–95.

1122 25. Zhou P, Silverstein KAT, Ramaraj T, Guhlin J, Denny R, Liu J, et al. Exploring structural variation and
1123 gene family architecture with De Novo assemblies of 15 *Medicago* genomes. *BMC Genomics.*
1124 2017;18:261.

1125 26. Fu H, Dooner HK. Intraspecific violation of genetic colinearity and its implications in maize. *Proc Natl
1126 Acad Sci U S A.* 2002;99:9573–8.

1127 27. Brunner S, Fengler K, Morgante M, Tingey S, Rafalski A. Evolution of DNA sequence nonhomologies
1128 among maize inbreds. *Plant Cell Online.* 2005;17:343.

1129 28. Schnable PS, Ware D, Fulton RS, Stein JC, Wei F, Pasternak S, et al. The B73 Maize Genome:
1130 Complexity, Diversity, and Dynamics. *Science*. 2009;326:1112–5.

1131 29. Pinkel D, Segraves R, Sudar D, Clark S, Poole I, Kowbel D, et al. High resolution analysis of DNA copy
1132 number variation using comparative genomic hybridization to microarrays. *Nat Genet*. 1998;20:207–11.

1133 30. Springer NM, Ying K, Fu Y, Ji T, Yeh C-T, Jia Y, et al. Maize Inbreds Exhibit High Levels of Copy Number
1134 Variation (CNV) and Presence/Absence Variation (PAV) in Genome Content. *PLoS Genet*.
1135 2009;5:e1000734.

1136 31. Hirsch CN, Hirsch CD, Brohammer AB, Bowman MJ, Soifer I, Barad O, et al. Draft Assembly of Elite
1137 Inbred Line PH207 Provides Insights into Genomic and Transcriptome Diversity in Maize. *Plant Cell*.
1138 2016;28:2700–14.

1139 32. Cooper GM, Zerr T, Kidd JM, Eichler EE, Nickerson DA. Systematic assessment of copy number
1140 variant detection via genome-wide SNP genotyping. *Nat Genet*. 2008;40:1199–203.

1141 33. Dellinger AE, Saw S-M, Goh LK, Seielstad M, Young TL, Li Y-J. Comparative analyses of seven
1142 algorithms for copy number variant identification from single nucleotide polymorphism arrays. *Nucleic
1143 Acids Res*. 2010;38:e105–e105.

1144 34. Wang X, Le Barbier E, Aubert J, Robin S. Variational Inference for Coupled Hidden Markov Models
1145 Applied to the Joint Detection of Copy Number Variations. *Int J Biostat*. 2019;15. doi:10/gf7323.

1146 35. Wang K, Li M, Hadley D, Liu R, Glessner J, Grant SFA, et al. PennCNV: An integrated hidden Markov
1147 model designed for high-resolution copy number variation detection in whole-genome SNP genotyping
1148 data. *Genome Res*. 2007;17:1665–74.

1149 36. Didion JP, Yang H, Sheppard K, Fu C-P, McMillan L, de Villena F, et al. Discovery of novel variants in
1150 genotyping arrays improves genotype retention and reduces ascertainment bias. *BMC Genomics*.
1151 2012;13:34.

1152 37. Unterseer S, Bauer E, Haberer G, Seidel M, Knaak C, Ouzunova M, et al. A powerful tool for genome
1153 analysis in maize: development and evaluation of the high density 600k SNP genotyping array. *BMC
1154 Genomics*. 2014;15:823.

1155 38. Hupé P, Stransky N, Thiery J, Radvanyi F, Barillot E. Analysis of array CGH data: from signal ratio to
1156 gain and loss of DNA regions. *Bioinformatics*. 2004.

1157 39. Olshen AB, Venkatraman ES, Lucito R, Wigler M. Circular binary segmentation for the analysis of
1158 array-based DNA copy number data. *Biostatistics*. 2004;5:557–72.

1159 40. Picard F, Robin S, Lavielle M, Vaisse C, Daudin J. A statistical approach for array CGH data analysis.
1160 *BMC Bioinformatics*. 2005;6:27.

1161 41. Picard F, Robin S, Le Barbier É, Daudin J. A segmentation/clustering model for the analysis of array
1162 CGH data. *Biometrics*. 2007;63:758–66.

1163 42. Marioni J, Thorne N, Tavare S. BioHMM: a heterogeneous hidden Markov model for segmenting
1164 array CGH data. *Bioinformatics*. 2006;22:1144.

1165 43. Stjernqvist S, Ryden T, Skold M, Staaf J. Continuous-index hidden Markov modelling of array CGH
1166 copy number data. *Bioinformatics*. 2007;23:1006.

1167 44. Lyra DH, Galli G, Alves FC, Granato ÍSC, Vidotti MS, Bandeira e Sousa M, et al. Modeling copy number
1168 variation in the genomic prediction of maize hybrids. *Theor Appl Genet*. 2018. doi:10.1007/s00122-018-
1169 3215-2.

1170 45. Alkan C, Coe BP, Eichler EE. Genome structural variation discovery and genotyping. *Nat Rev Genet*.
1171 2011;12:363–376.

1172 46. Chen K, Wallis JW, McLellan MD, Larson DE, Kalicki JM, Pohl CS, et al. BreakDancer: an algorithm for
1173 high-resolution mapping of genomic structural variation. *Nat Methods*. 2009;6:677–81.

1174 47. Kidd JM, Cooper GM, Donahue WF, Hayden HS, Sampas N, Graves T, et al. Mapping and sequencing
1175 of structural variation from eight human genomes. *Nature*. 2008;453:56–64.

1176 48. Korbel JO, Urban AE, Affourtit JP, Godwin B, Grubert F, Simons JF, et al. Paired-End Mapping Reveals
1177 Extensive Structural Variation in the Human Genome. *Science*. 2007;318:420–6.

1178 49. Tuzun E, Sharp AJ, Bailey JA, Kaul R, Morrison VA, Pertz LM, et al. Fine-scale structural variation of
1179 the human genome. *Nat Genet*. 2005;37:727–32.

1180 50. Ye K, Schulz MH, Long Q, Apweiler R, Ning Z. Pindel: a pattern growth approach to detect break
1181 points of large deletions and medium sized insertions from paired-end short reads. *Bioinformatics*.
1182 2009;25:2865–71.

1183 51. Lai J, Li R, Xu X, Jin W, Xu M, Zhao H, et al. Genome-wide patterns of genetic variation among elite
1184 maize inbred lines. *Nat Genet*. 2010;42:1027–30.

1185 52. The Danish Pan-Genome Consortium, Sibbesen JA, Maretty L, Krogh A. Accurate genotyping across
1186 variant classes and lengths using variant graphs. *Nat Genet*. 2018;50:1054–9.

1187 53. Muñoz-Amatriaín M, Eichten SR, Wicker T, Richmond TA, Mascher M, Steuernagel B, et al.
1188 Distribution, functional impact, and origin mechanisms of copy number variation in the barley genome.
1189 *Genome Biol*. 2013;14:R58.

1190 54. Ganal MW, Durstewitz G, Polley A, Bérard A, Buckler ES, Charcosset A, et al. A Large Maize (*Zea mays*
1191 L.) SNP Genotyping Array: Development and Germplasm Genotyping, and Genetic Mapping to Compare
1192 with the B73 Reference Genome. *PLoS ONE*. 2011;6:e28334.

1193 55. Bouchet S, Servin B, Bertin P, Madur D, Combes V, Dumas F, et al. Adaptation of maize to temperate
1194 climates: mid-density genome-wide association genetics and diversity patterns reveal key genomic
1195 regions, with a major contribution of the *Vgt2* (*ZCN8*) locus. *PloS One*. 2013;8:e71377.

1196 56. Bouchet S, Bertin P, Presterl T, Jamin P, Coubranche D, Gouesnard B, et al. Association mapping for
1197 phenology and plant architecture in maize shows higher power for developmental traits compared with

1198 growth influenced traits. *Heredity*. 2016.
1199 <https://www.nature.com/hdy/journal/vaop/ncurrent/full/hdy201688a.html>. Accessed 21 Jun 2017.

1200 57. Camus-Kulandaivelu L. Maize Adaptation to Temperate Climate: Relationship Between Population
1201 Structure and Polymorphism in the Dwarf8 Gene. *Genetics*. 2006;172:2449–63.

1202 58. Gabur I, Chawla HS, Snowdon RJ, Parkin IAP. Connecting genome structural variation with complex
1203 traits in crop plants. *Theor Appl Genet*. 2019;132:733–50.

1204 59. Feschotte C, Jiang N, Wessler SR. PLANT TRANSPOSABLE ELEMENTS: WHERE GENETICS MEETS
1205 GENOMICS. *Nat Rev Genet*. 2002;3:329–41.

1206 60. Morgante M, De Paoli E, Radovic S. Transposable elements and the plant pan-genomes. *Curr Opin
1207 Plant Biol*. 2007;10:149–55.

1208 61. Ducrocq S, Madur D, Veyrieras JB, Camus-Kulandaivelu L, Kloiber-Maitz M, Presterl T, et al. Key
1209 impact of Vgt1 on flowering time adaptation in maize: evidence from association mapping and
1210 ecogeographical information. *Genetics*. 2008;178:2433–7.

1211 62. Salvi S, Sponza G, Morgante M, Tomes D, Niu X, Fengler KA, et al. Conserved noncoding genomic
1212 sequences associated with a flowering-time quantitative trait locus in maize. *Proc Natl Acad Sci U A*.
1213 2007;104:11376–81.

1214 63. Salvi S, Tuberosa R, Chiapparino E, Maccaferri M, Veillet S, van Beuningen L, et al. Toward positional
1215 cloning of Vgt1, a QTL controlling the transition from the vegetative to the reproductive phase in maize.
1216 *Plant Mol Biol*. 2002;48:601–613.

1217 64. Clark AG, Hubisz MJ, Bustamante CD, Williamson SH, Nielsen R. Ascertainment bias in studies of
1218 human genome-wide polymorphism. *Genome Res*. 2005;15:1496–1502.

1219 65. Gouesnard B, Negro S, Laffray A, Glaubitz J, Melchinger A, Revilla P, et al. Genotyping-by-sequencing
1220 highlights original diversity patterns within a European collection of 1191 maize flint lines, as compared
1221 to the maize USDA genebank. *Theor Appl Genet*. 2017. doi:10.1007/s00122-017-2949-6.

1222 66. Gore MA, Chia JM, Elshire RJ, Sun Q, Ersoz ES, Hurwitz BL, et al. A first-generation haplotype map of
1223 maize. *Sci Wash*. 2009;326:1115–7.

1224 67. Brandenburg J-T, Mary-Huard T, Rigail G, Hearne SJ, Corti H, Joets J, et al. Independent introductions
1225 and admixtures have contributed to adaptation of European maize and its American counterparts. *PLOS
1226 Genet*. 2017;13:e1006666.

1227 68. Yeaman S. Genomic rearrangements and the evolution of clusters of locally adaptive loci. *Proc Natl
1228 Acad Sci*. 2013;110:E1743–51.

1229 69. Gu W, Zhang F, Lupski JR. Mechanisms for human genomic rearrangements. *PathoGenetics*.
1230 2008;1:4.

1231 70. Li H, Handsaker B, Wysoker A, Fennell T, Ruan J, Homer N, et al. The Sequence Alignment/Map
1232 format and SAMtools. *Bioinformatics*. 2009;25:2078–9.

1233 71. Quinlan AR, Hall IM. BEDTools: a flexible suite of utilities for comparing genomic features.
1234 *Bioinformatics*. 2010;26:841–2.

1235 72. Gnerre S, MacCallum I, Przybylski D, Ribeiro FJ, Burton JN, Walker BJ, et al. High-quality draft
1236 assemblies of mammalian genomes from massively parallel sequence data. *Proc Natl Acad Sci.*
1237 2011;108:1513–8.

1238 73. Waterhouse RM, Seppey M, Simão FA, Manni M, Ioannidis P, Klioutchnikov G, et al. BUSCO
1239 Applications from Quality Assessments to Gene Prediction and Phylogenomics. *Mol Biol Evol.*
1240 2018;35:543–8.

1241 74. Altschul SF, Gish W, Miller W, Myers EW, Lipman DJ. Basic local alignment search tool. *J Mol Biol.*
1242 1990;215:403–10.

1243 75. Abyzov A, Gerstein M. AGE: defining breakpoints of genomic structural variants at single-nucleotide
1244 resolution, through optimal alignments with gap excision. *Bioinformatics*. 2011;27:595–603.

1245 76. Gremme G, Steinbiss S, Kurtz S. GenomeTools: A Comprehensive Software Library for Efficient
1246 Processing of Structured Genome Annotations. *IEEE/ACM Trans Comput Biol Bioinform.* 2013;10:645–
1247 56.

1248 77. Tai TH, Tanksley SD. A rapid and inexpensive method for isolation of total DNA from dehydrated
1249 plant tissue. *Plant Mol Biol Report.* 1990;8:297–303.

1250 78. Dellaporta SL, Wood J, Hicks JB. A plant DNA minipreparation: Version II. *Plant Mol Biol Report.*
1251 1983;1:19–21.

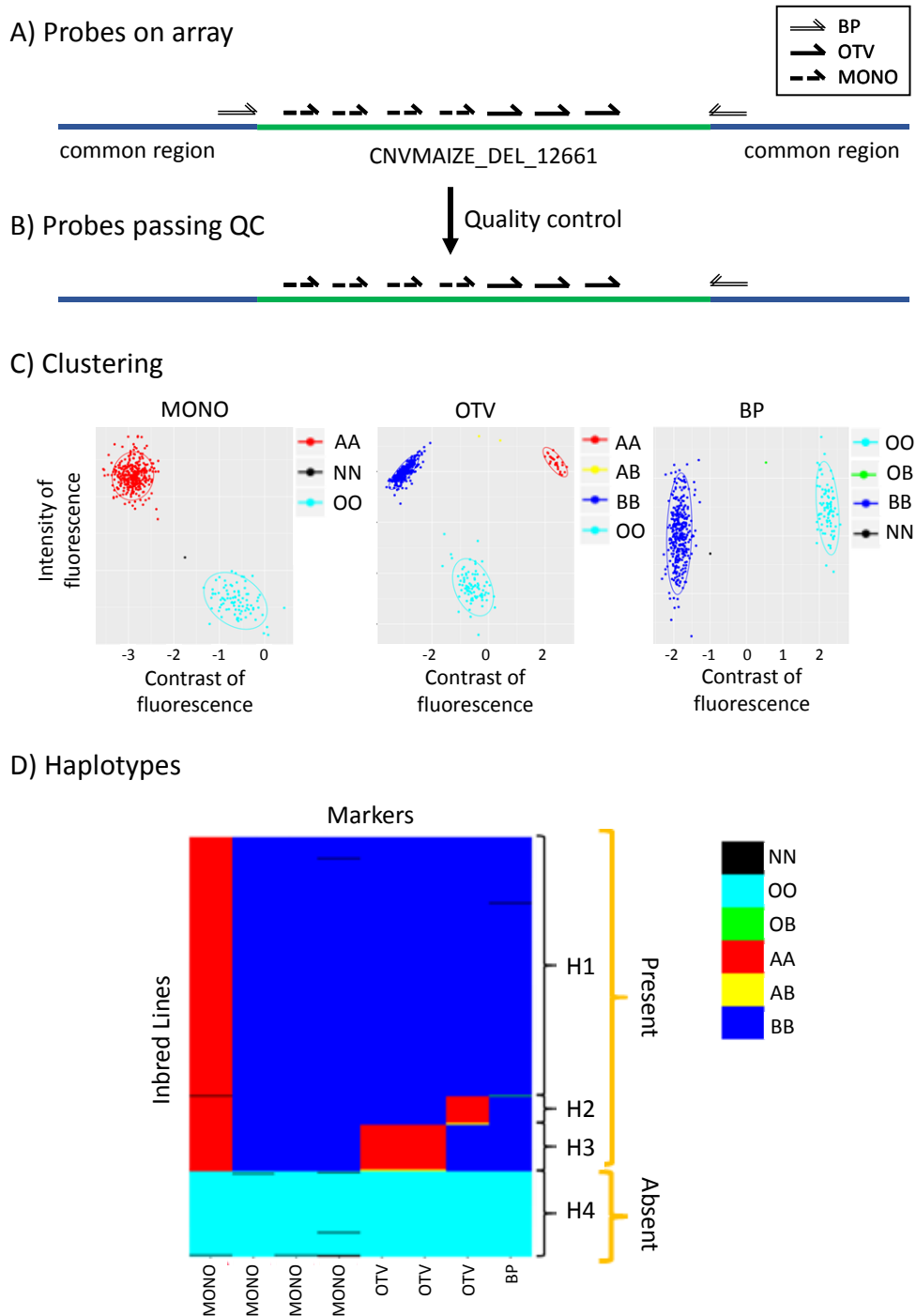
1252 79. Aulchenko Y. GenABEL: an R package for Genome Wide Association Analysis. 2009.

1253 80. Alexander DH, Novembre J, Lange K. Fast model-based estimation of ancestry in unrelated
1254 individuals. *Genome Res.* 2009;19:1655–64.

1255

1256 **Figures**

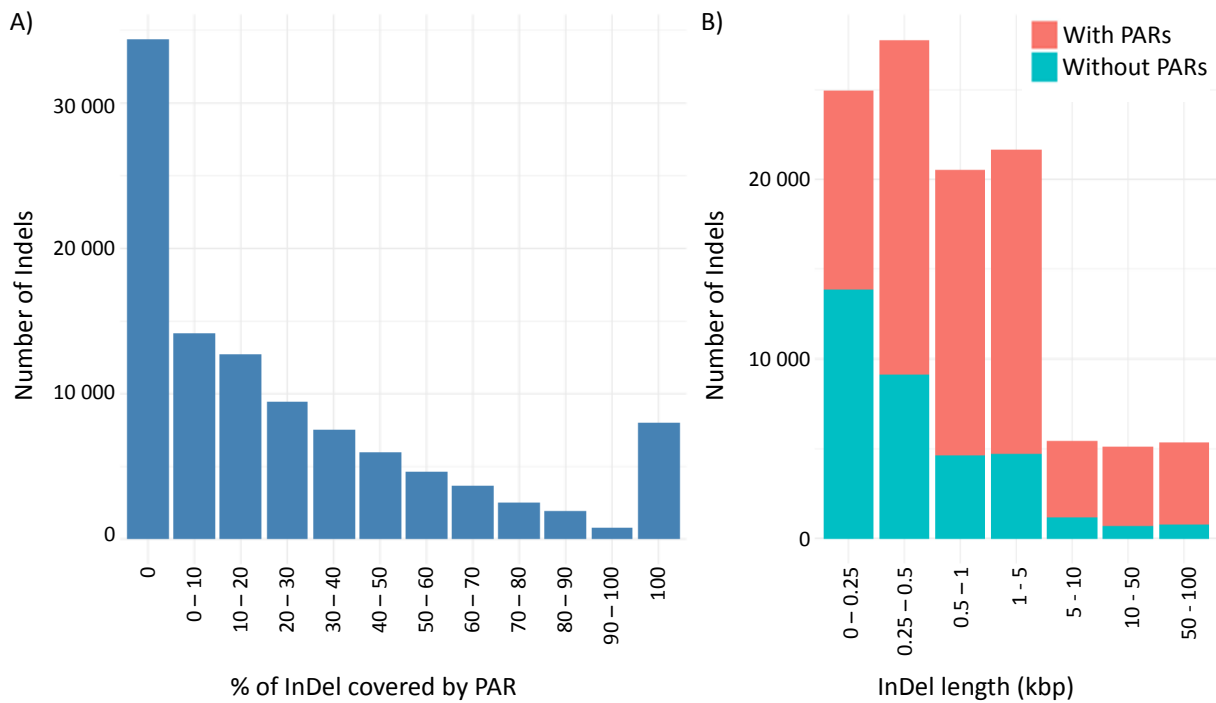
1257 **Figure 1:** Genotyping of InDel CNVMAIZE_DEL_12661 using three probe types on 445 individuals. A)
1258 Schematic distribution of the 9 probes along the sequence of InDel CNVMAIZE_DEL_12661 (green line)
1259 and the bordering sequence common between all individuals (blue line) genotyped by the array. Double,
1260 dotted, and full arrows represented the probes designing on the forward and reverse flanking sequences
1261 of the breakpoint sites (BP), at not polymorphic (MONO) and polymorphic sites (OTV) within internal
1262 sequence of InDel. B) Schematic distribution of the 8 probes passing Affymetrix® quality control and called
1263 by the Affymetrix® pipeline C) Clustering produced by the Affymetrix® algorithm for an OTV, MONO, and
1264 BP probe from InDel based on both fluorescence contrast (X axis) and intensity (Y axis) of the 445 inbred
1265 lines. Red, blue and yellow dots indicated the presence of the sequence (genotype “present”) either
1266 homozygous for allele A (AA) or allele B (BB) or heterozygous (AB), respectively. Cyan and green indicated
1267 that the sequence was absent in the individual (OO), or only in one copy of the sequence, e.g hemizygous
1268 for presence/absence (OB or OA). Black dots indicated individuals for which no genotype could be
1269 assigned (Missing data) D) Haplotypes displayed by the genotyping using 8 probes (column) on the 445
1270 inbred lines (row). Colors corresponded to the genotype of individuals produced by clustering in C)



1271

1272

1273 **Figure 2:** Distribution of 105,927 InDels genotyped by the array according to their size and the cumulated
1274 length of Presence/Absence regions (PARs) in their internal sequence. A) Distribution of the number of
1275 InDels according to the proportion of presence/absence regions (sequence not present elsewhere in the
1276 genome) within their internal sequence. B) Distribution of the number of InDels according to their size
1277 (kbp) and the percentage of internal sequence of InDel covered by PAR(s). Red Color indicates the
1278 proportion of InDels with (red) or without (blue) PARs for the 7 InDel size classes.

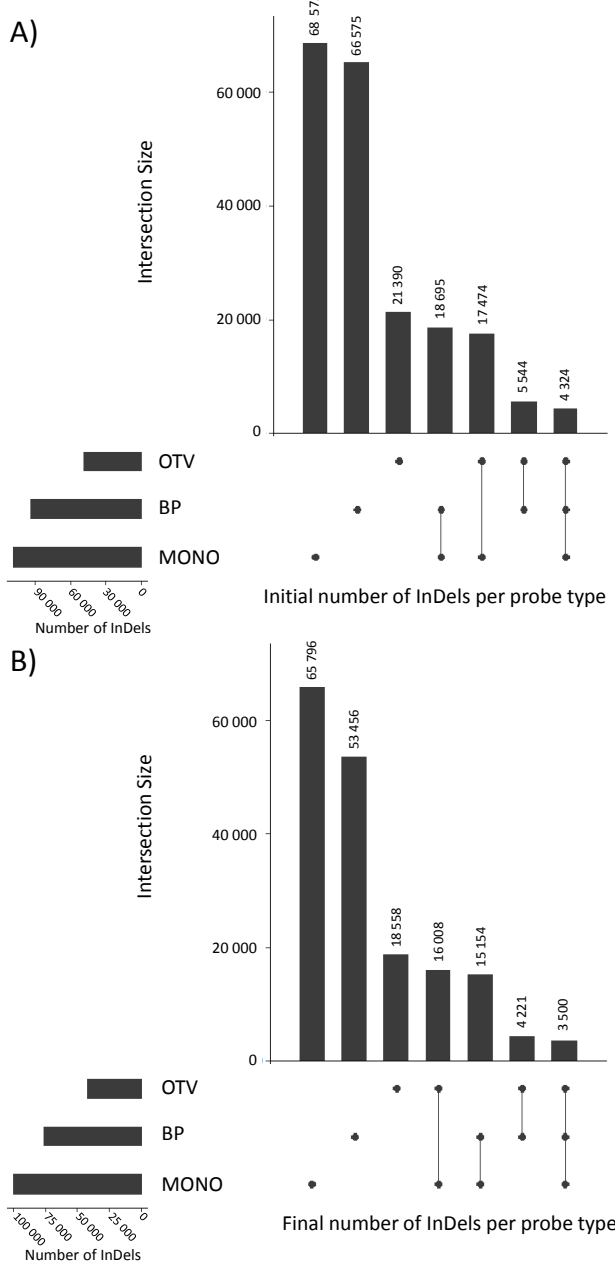


1279

1280

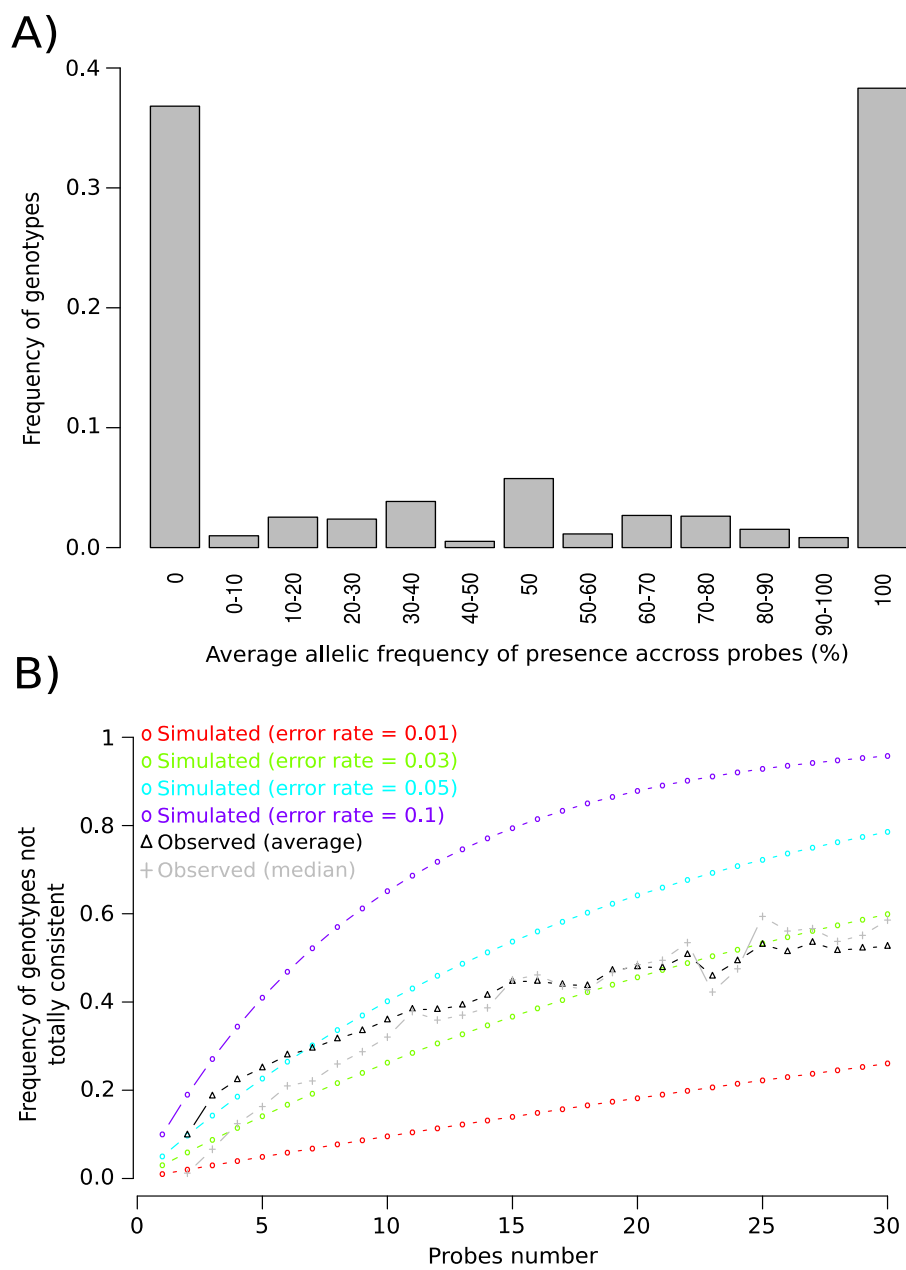
1281

1282 **Figure 3:** Number of InDels interrogated by each probe types or their combination, for which: a probe
1283 could be designed (A) and a probe was finally selected to be included in the final array (B). Vertical bars
1284 indicate number of InDels interrogated by each probe types or their combination. Black points and
1285 connected traits below the vertical bars indicate the corresponding probes types or their combination
1286 that are used for interrogating this subset of InDels. Horizontal bars indicate number of InDels
1287 interrogated by each probe types (OTV, BP, MONO). Number of InDels by probe type, for which: a probe
1288 could be designed (A) and a probe was finally selected to be included in the final array (B). Number of
1289 InDels that could be targeted by each type of probes designed (A) and selected to be included in the final
1290 array (B).



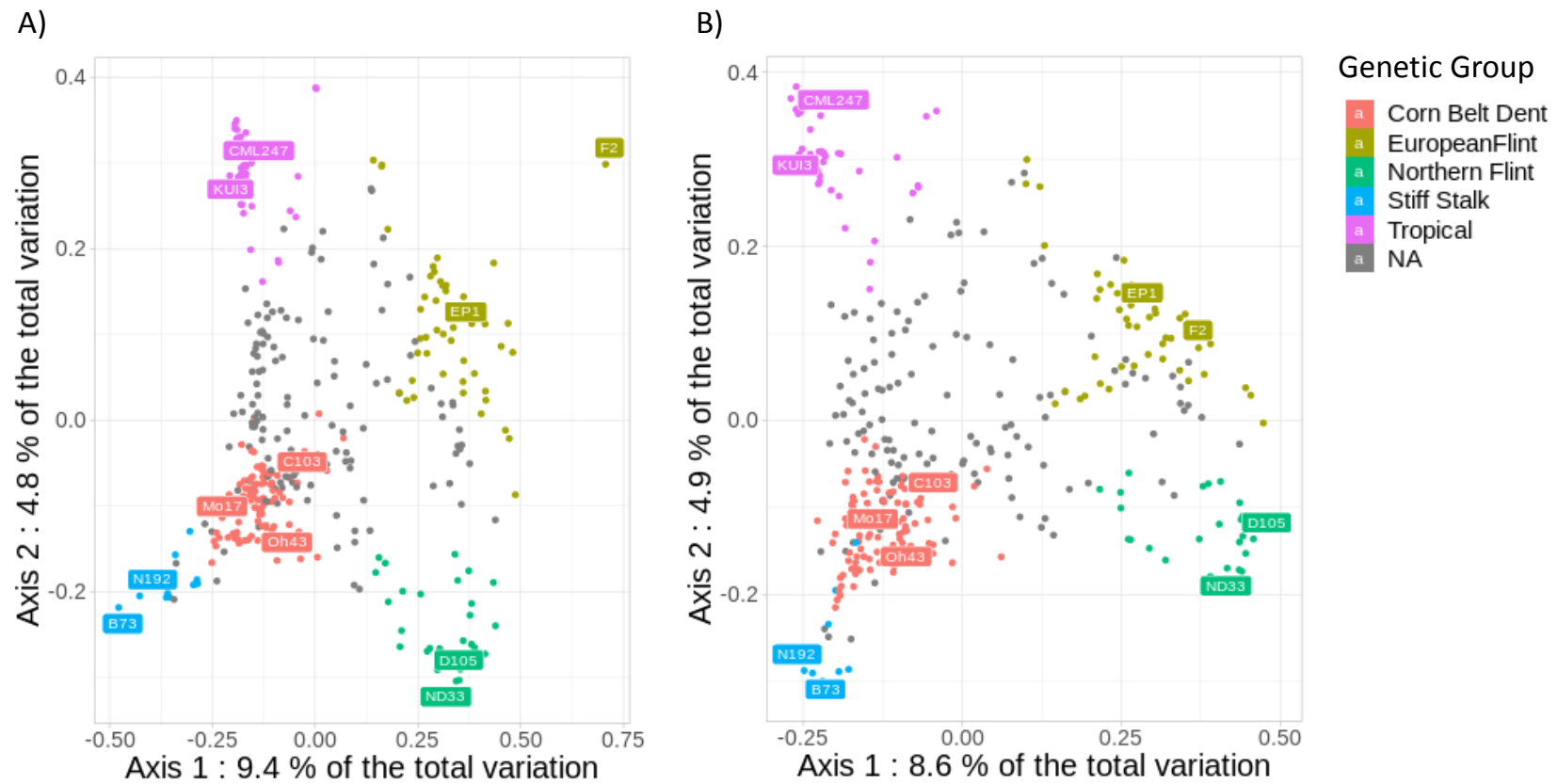
1291

1292 **Figure 4:** Consistencies among probes within 50,648 InDels with at least two probes genotyped in 362
1293 inbred lines. (A) Distribution of the average allelic frequencies of present calls over all probes. (B) Variation
1294 of proportion of genotypes not fully consistent across all probes. The black and gray curves with triangle
1295 points represent the variation of the median and average FreqDiff01 across InDels, respectively. Colored
1296 curves with circle points represent the expected variation of the proportion for different error rates (1%:
1297 red, 3%: green, 5%: light blue, 10%: dark blue). Frequencies of 1 (presence) and 0 (absence) indicate that
1298 all probes had consistent genotypes for the corresponding inbred line. Intermediate frequencies
1299 (FreqDiff01) indicate that at least one probe was not consistent with the other probes for the same InDel
1300 in one inbred line.



1301

1302 **Figure 5:** Principal coordinate analysis on the genetic distance between 362 inbred lines from an association panel estimated by A) 57,824 InDels
1303 and B) 28,143 SNPs. Colors represent the assignment of the inbred lines to the 5 genetic groups defined by admixture using pre-fixed Panzea SNPs
1304 from the 50K Illumina array, when the probability of assignment to a group (membership) was greater than 60%. Inbred lines not assigned to a
1305 group were considered admixed and colored gray. The common names of maize accessions, typical of each genetic group, were used.



1306

1307

1308

1309

Additional Files

1310

Additional file 1:

1311

Table S1: Summary of sequencing data used during the assembly process provided by ALLPATHS-LG; **Table S2:** Classification by the Affymetrix® pipeline of 84,994 BP probes based on cluster number, separation, variance, and call rate. A) Probes recommended for genotyping, B) Probes not recommended for genotyping; **Table S3:** Classification by the Affymetrix® pipeline of 163,278 OTV probes based on cluster number, separation, variance, and call rate. A) Probes recommended for genotyping B) Probes not recommended probes for genotyping; **Table S4:** Classification by the Affymetrix® pipeline of 414,500 MONO probes, based on cluster number, separation, variance, and call rate. A) Probes recommended for genotyping B) Probes not recommended for genotyping; **Table S5:** Effect of probe number within InDels on average percentage of missing data, of genotypes absent and genotypes not fully concordant; **Table S6:** Simulation of genotyping error rates for 362 lines and 10,000 InDels called by various numbers of probes with a probe genotyping error rate ranging from 1% to 10%; **Table S7:** Comparison of reproducibility between 5 DNA replicates of hybrid F1 according to probes type and observed clustering; **Table S8:** Mendelian inheritance of 12 hybrids F1 derived from 9 different parental inbred lines for 46,382 BP probes passing Affymetrix quality control and polymorphic; **Table S9:** Comparison of the reproducibility of InDels and SNP genotyping between 13 maize varieties replicated on 50K Illumina SNP and Affymetrix® Axiom® InDel arrays

1323

Additional file 2:

1324

Figure S1: Description of two approaches used to discover InDels using resequencing data of DNA; **Figure S2:** Number and complementarity of A) deletions and B) insertions regarding B73 reference genome discovered between F2, PH207 and C103 inbred lines and B73; **Figure S3:** Schematic representation of four different breakpoint types identified by PINDEL at InDel breakpoints according to the presence of micro-homology sequence or not in place of the deleted sequence; **Figure S4:** Distribution of probe number per InDel for 105,927 InDels genotyped with the array; **Figure S5:** Relationship between probes number genotyping the InDel and A) the InDel length B) cumulated length of specific sequence (PARs) within InDel; **Figure S6:** Variation of probes and InDels density across the 10 maize chromosomes; **Figure S7:** Three dedicated Affymetrix pipelines used for calling InDel polymorphisms from the fluorescent intensity variation of BP probes (A), OTV probes (B) and MONO probes (C); **Figure S8:** Example of clustering based on probes fluorescence (intensity in y-axis and contrast in x-axis), for 14 different classifications of probes assigned by the Affymetrix® algorithm; **Figure S9:** Example of clustering for 6 randomly probes in different classifications; **Figure S10:** Variation of the distribution of the average consistency rate (%) of InDels between expected and observed genotyping of probes according to number of probes within the InDel; **Figure S11:** Haplotype of two InDels genotyped with multiple probes (in column) for 362 individuals (in rows); **Figure**

1335 **S12:** Effect of average frequency of absence across 362 lines on consistencies between probes genotyping within InDels; **Figure S13:** Comparison
1336 of kinship between 362 inbred lines estimated with 57,824 InDels and with 28,143 SNPs from the 50K Illumina genotyping array; **Figure S14:**
1337 Principal coordinate analysis on the genetic distance between 360 inbred lines from an association panel (B73 and F2 were excluded) estimated
1338 by A) 57,824 InDels and B) 28,143 SNPs.